GIMA
Geographical Information Management and Applications

Assessing River Dynamics Using a Timeseries of UAV Imagery

A case study of the Petit Buëch river in Hautes – Alpes, Southern France

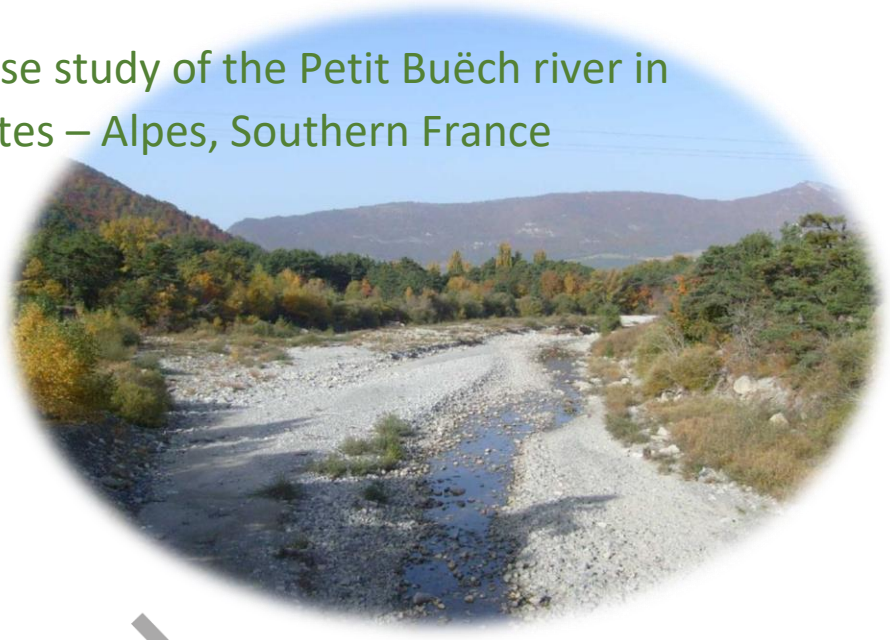

Luca Petrone - 6148336 - l.petrone@students.uu.nl

Geographic Information Management and Application - Faculty of Geosciences - Utrecht University

1st Supervisor: Drs. M. Zeylmans Van Emmichoven

2nd Supervisor: Prof. Dr. S. M. De Jong

Acknowledgements

This master thesis is the end of long journey started in September 2017. This would not be possible without help of my family, who always sustained me and helped me to achieve this milestone.

I would like also to express my gratitude to my two supervisors: Prof. Dr. Steven De Jong, who gave me the topic and all the data to work with and precious suggestions on what to read for better understanding river dynamics.

Drs. Maarten Zeylmans Van Emmichoven, who pointed me to Prof. Dr. Steven De Jong, supported me in all the technical aspects of the project and enthusiastically shared with me his passion for photogrammetry. Also thank you for the free coffee.

To both, thank you for the feedback, the help with all the setbacks encountered and the trial presentations before the defenses.

Lastly, I would like to thank all my friend and peers that helped me, shared thoughts and supported me in these months: Eoin, for the English proof reading and final feedback, constant support and for being among the few that appreciated my maps. Tobias, my Agisoft Photoscan buddy, who knows how it feels waiting for each process to end, thank you for the all the support and relief given in those long boring session looking at that green bar slowly filling. Guillermo, for pushing me in giving the best throughout these two years.

Abstract

The start of photogrammetry can be dated back to the XIX century, but this field has seen a narrow development for almost 150 years, attributable to the poor results obtained despite the huge resources required to achieve them. The digitization of the data and digital acquisition of the aerial imagery led, in the last 20 years, to a fast development of photogrammetric techniques, increasing the quality of data obtained while enormously reducing the costs. In this context, the use of Unmanned Airborne Vehicles (UAVs) is the natural evolution of 150 years of aerial photography.

The Petit Buëch is a highly dynamic river system in the south-east of France, with a clear braiding pattern. The erosion of the two catchments studied, at Le Pont du Chabestan and La Bâtie-Montsaléon, is high and endangers nearby anthropic structure and infrastructure. Thus, studying its dynamics is of pivotal importance. In order to monitor and study these dynamics, a series of photos captured by an Unmanned Airborne Vehicle (UAV) will be used, processed and analysed through the application of photogrammetric techniques.

The two study areas have already two sets of photos processed and analysed (2014 and 2015), from a previous work in the same area, and these sets will be integrated with the latest available photography from 2016 and 2017. With Agisoft PhotoScan and the Structure-from-Motion algorithm, the imagery will be processed and yield two OrthoMosaics and two Digital Elevation Models (DEMs) that will be finally used to carry out a qualitative and quantitative analysis of the two areas.

The qualitative analysis will concern the visual comparison of the two OrthoMosaic from 2016 and 2017, seeking for clear river path change and bank displacement. The quantitative analysis will try to quantify this displacement through a profile analysis of the river in 2016 and 2017, while a volume change analysis will consider also the DEMs from 2014 and 2015.

The goal of this thesis project is to understand the river dynamics of the Petit Buëch but also the accuracy and quality of the product delivered in the end. It is noteworthy that the UAV and camera used to capture the imagery were not high-end, posing interesting questions on how cheap tools perform and how high quality the products they yield could be.

Table of Contents

LIST OF TABLES

LIST OF FIGURES

1 Introduction

This study proposes to study and analyse the behaviour of the river bank of the Petit Buëch River in the Hautes-Alpes region, southern France. Rivers, despite being only 0.0002% of the total water present on Earth and 0.006% of the freshwater available to humanity (USGS, 2018), have played a pivotal role in the development and growth of human societies. Therefore, river management has always been a major concern for human populations. dredging, snagging and clearing, artificial levees and embankments, bank and bed protection, dams and locks are clear examples of how populations have tried, over the course of centuries, to transform and control rivers (Charlton, 2007).

Using UAV imagery, two catchments of the Buëch river will be studied. The imagery will be processed in Agisoft PhotoScan, a fascinating program that uses the Structure-from-Motion algorithm to reconstruct 3D models out of still imagery. The expected outputs of this research are, essentially, two: on one hand, the results obtained by processing the available dataset and, on the other hand, the comparison with the results obtained by Hemmelder et al. (2018). Therefore, this will yield to a total of five expected products in the end of the research. The 2016 and 2017 datasets will result in:

- Two OrthoMosaics for the river sections studied, at a precision in the order of ~5 cm;
- The derived DEMs, at a precision of ~10 cm;

Whereas, a comparison with Hemmelder et al. (2018) results will produce:

- A river bank erosion map between 2014 – 2017 and the estimated volume displaced;
- A map illustrating the morphological changes between 2014 – 2017.

2 Research Objectives

The thesis objective, as previously stated, is to study the behaviour of the Petit Buëch river and understand how appropriate the chosen photogrammetry techniques are. The thesis proposes to investigate two subjects interrelated with each other, one focusing on geographic information technology while the other that investigates the physical aspects and dynamics of the river itself.

Firstly, the main goal is to study and evaluate the efficiency of using UAV data for studying bank erosion and bank movement. The focus will be on the quality achievable, the speed of data processing, its viability and reproducibility in different context and domain of the derived product (the OrthoMosaic and OrthoDEM). Moreover, it will be studied the importance of using GIS techniques in the creation of time-series and up to date maps of critical areas, if any, where river morpho-dynamics are derived.

Secondly, river dynamics are studied. This is directly influenced by the results obtained in the processing of the UAVs data and aims to analyse the behaviour of the Petit Buëch by looking in the strength of the change, if any, of its path, the bank erosion and the possible threat for nearby human activities.

A series of research questions have been outlined below to easily understand the research objectives and how the study will be carried on:

1. **How the creation of a DEM, the related OrthoPhoto and 3D model can help with river bank analysis?**

    1.1. Is 'Agisoft PhotoScan' workflow the best approach for 3D mapping and DEM construction?

    1.2. How can the quality of the obtained products and what is the accuracy of the obtained products be assessed?

    1.3. Does using oblique images raise any problem in data processing or may be an advantage for the resulting 3D model?

2. **What is the behaviour of the river bank?**

    2.1. Is there any change in the morphology of the river between 2016 and 2017?

    2.2. If any, is it stronger than previous years?

    2.3. Is it a threat to human activity?

    2.4. Is the river area subjected to mass soil loss and, if so, is it quantifiable?

2.1 What is out of scope

Out of scope of this study is the finding of a solution for soil loss. The main scope of this study is to develop a monitoring method using drone imagery, which is extremely accurate, cheaper than classic aerial photography/LiDAR systems and provides a high-quality final product that will have scientific value but also, hopefully, a practical value for river and land administrations.

3 River processes

3.1 Discharge and runoff generation

Before diving into detail in the study area and the problem connected to bank erosion, a compliant excursus on river processes has to be done, to have a clear overview on why and how the hydrological problems affecting this area form.

Most of the water in rivers originates as precipitation. A system of inputs, outputs, storages and transfers represent the main elements of a drainage basin hydrology. The movement of water above and below the surface can be, loosely, defined as runoff (Charlton, 2007). A more precise definition of runoff, or basin channel runoff, is the quantity of water that enters in a drainage basin in a defined limit of time and can be find out by a water-balance equation, where precipitation represents runoff and the losses through evapotranspiration changes in the amount of soil moisture and ground water storage (Summerfield, 1991).

Channel discharge differs over time and space on different scales. Its changes over time are represented by a hydrograph plotted against time. However, the direct measurement of discharge is time-consuming, therefore it is estimated from stage hydrograph. Here, the variation is showed in stage (the elevation of water surface) through time and the changes are plotted in a stage-discharge rating curve, which plots changes in discharge against changes in water depth (Summerfield, 1991). Discharge is usually expressed in m^3s^{-1}, but it may be more appropriate express it as mean depth of water over basin and a common index can be obtained by dividing mean annual discharge by the drainage basin area (e.g. from <31mm of the Colorado River to >1000mm of the Amazon River).

Discharge of rivers may be influenced by spatial and/or temporal variations. Usually, as tributary rivers gradually add runoff to the main stem, discharge increases downstream. On a higher, global, scale river discharge is strictly correlated to the balance between precipitations and evotranspiration, in fact the highest discharges are recorded in rivers flowing in extremely humid environments (Summerfield, 1991).

Temporal variation, meanwhile, are clear in environments with strong seasonal variation in precipitation or temperature. Stream flow is inclined to vary quite regularly over the year and these average annual variations are referred as river regime. Of great importance are also the factors that determine these variations in the discharge of streams draining relatively small drainage basins (Summerfield, 1991). These small basins normally show a stable discharge sustained by groundwater flow, defined as base flow, interrupted by precipitation events plotted as storm hydrographs, the shape of which depend on a number of interrelated factors such as intensity, duration, areal extent and the hydrological properties of the basin (Charlton, 2007; Summerfield, 1991).

The mean frequency of floods can be estimated in two ways: (1) it can be ranked the highest discharge of each year, producing an annual series. The interval is given by (n+1)/r, where 'n' is number of recorded years and 'r' is the rank order of the flood of the specified magnitude. (2) otherwise, using partial duration series, by listing and rating all discharges, over a precise extent of time, which exceeded a particular magnitude (Summerfield, 1991). By mean annual flood is defined the flood that is at least equal in magnitude to the mean flood in annual series, while the most probable annual flood, in general, appears to be approximately correspondent in magnitude to bankfull discharge, that is the maximum flow that can be contained in a channel before filling its capacity.

The generation of runoff depends on different water contribution to the stream flow. This flow can be divided into two distinct kinds, according to the rapidity it enters the stream channel after a storm: delayed flow or quick flow. In drainage basins lacking major vegetation cover, soil infiltration capacity may be low enough to be topped by precipitation strengths during stormy events. Once the surface is at full capacity, infiltration-excess overland flow will be generated, known as partial area model of stream flow generation. Meanwhile, in well-vegetated basins the saturated zones initially expand with the beginning of the rainfall event and then contract once it stops. This known as a variable source model. Also, lateral movement of water through the soil itself are important for quick flow, as this is most distinct just above the soil with a lower hydraulic conductivity. Runoff reaction to a storm event is also influenced by other different properties of the drainage system or morphological

characteristics of the basin, like density of the channel, basin relief and its shape. These factors influence the arrival time of runoff from tributaries to the main trunk (Charlton, 2007; Summerfield, 1991).

3.2 Channel creation and flow regimes

How does a channel originate? Flows on the surface, and below it, converge in areas of concave relief, and this is a crucial factor in the development of the channel. In semi-arid contexts, infiltration-excess overland flow can lead to the development of rills; however, the mechanism is not yet fully clear. In humid environments, channel initiation is likely to be ideal where subsurface natural pipes are present. Spring sapping could also be source for creating new channels. Ground water flow is amassed in more permeable areas in the bedrock, encouraging chemical erosion of the bedrock and therefore leading to an increase in the hydraulic conductivity. Spring sapping is expected to be particularly effective where a permeable lithology (like sandstone or limestone) covers an impermeable lithology (like clay) (Summerfield, 1991).

In channel there are two contrasting forces that act on the flow of water. The driving force is gravity (downslope direction), while the resisting force occurs from friction energy, within the body of water and between the flowing water and the channel surface. The ability of water to transport material is determined by these two forces.

Resistance of a fluid is represented by its viscosity. One type of resistance occurs from internal friction caused by cohesion and collisions between molecules as they move past each other, and this is known as molecular viscosity or dynamic viscosity.

Fluids have several types of flows according to their viscosity. For example, lava (which has high viscosity) motion is described as laminar flow, like series of thin layers are sliding over one another. However, this is quite rare for water flows, where typically the flow is defined as turbulent, since the flow motion is in every direction within the fluid. Usually, there is a laminar sublayer within which the speed of flow initially increases linearly, while above this sublayer the rate of increase flow speed is roughly logarithmic (Charlton, 2007; Summerfield, 1991).

Mean flow velocity, molecular viscosity, density of the fluid and the dimensions of the flow section determine if the flow is laminar or turbulent. The hydraulic radius, which is a measure of channel efficiency defined by the ratio between cross-sectional area and wetted perimeter, is used for stream channels to determine the dimension of the flow section. To determine when laminar or turbulent flow arise, a Reynolds number (*Re*), which is a dimensionless measure of flow rate, is used. This number is obtained by multiplying the mean flow velocity (v) and hydraulic radius (R) and dividing by the kinematic viscosity, which is a ratio between molecular viscosity and fluid density (Charlton, 2007).

$$Re = \frac{vR}{v}$$

Irregularities in channel bed create waves which exercise a weight. The ratio of the mean flow velocity (v) to the velocity of these gravity waves (g is acceleration gravity; d is depth of flow) defines the Froude number (*F*) of the flow and it can be used to distinguish various flow states.

$$F = \frac{v}{\sqrt{gd}}$$

When this number is less than 1, the wave velocity is greater than the mean flow velocity and is defined as subcritical (e.g. the ripples propagated by a stone thrown into a stream can travel upstream). When F number is 1 is defined as critical, while greater than 1 is supercritical (Charlton, 2007).

Changes in discharges can be achieved by variations in the depth and velocity of flow. Changes between subcritical and supercritical flow are regulated by flow velocity. A sudden change is described as hydraulic jump (from supercritical to subcritical) or hydraulic drop (vice versa). This can occur where there is an abrupt change in channel bed form, for example it is common in mountain streams. In natural channels, the mean F number

rarely go beyond 0.5 and supercritical flows are provisional. These two numbers can be combined to distinct four different flow regimes: subcritical laminar/ turbulent and supercritical laminar/turbulent flow (Summerfield, 1991).

To calculate the velocity of stream flows it must be remembered that it is affected by the gradient, roughness and cross-sectional form of the channel. There are two equations that are mainly used to calculate it:

Chezy equation

$$v = C\sqrt{Rs}$$

where 'C' is Chezy coefficient (gravitational and frictional forces), 'R' is hydraulic radius and 's' is the channel gradient. (cit. Charlton)

Manning equation (which is a more widely applied estimator)

$$v = \frac{R^{0.67}s^{0.5}}{n}$$

Where 'R' is hydraulic radius, 's' is channel gradient and 'n' is Manning roughness coefficient (usually estimated from tables) (cit. Charlton). Its use is might be problematic, because the resistance to flow changes with discharge and flow depth. It decreases as flow depth increases up to bankfull discharge. Once the capacity is topped, the flow spreads over a much larger area and the 'n' value increases (Summerfield, 1991).

3.3 Erosion and sediment transport

What has been seen so far brings us to one of the main problems associated with rivers and their management. Fluvial erosion reduces the landscape and might create serious threats to the environment and anthropic structures. It is important to understand the processes behind erosion, as the following processes are common in mountainous areas (Whipple, Hancock, & Anderson, 2000). Three major processes operate (Charlton, 2007; Summerfield, 1991):

- **Corrosion**: the chemical dissolution of minerals in contact with water.
- **Abrasion** (or **corrasion**): Mechanical wearing or detachment of rock by sediment moved by the water flow. Its effectiveness depends on the concentration, hardness and kinetic energy of the impacting particles and the resistance of the bedrock surface. Rates of abrasion increase rapidly as flow velocities increase.
- **Cavitation**: an acceleration of flow in a fluid causes a drop in pressure which, if of enough magnitude, leads to the formation of bubbles. Cavitation occurs when these bubbles implode and emit tiny jets of water at velocities that can generate stresses enough to fracture solid rock.

By entrainment it is defined the process to set in motion a solid particle in a fluid (Charlton, 2007). This happens when the pressures acting on a particle exceed the resisting forces, which are the immersed weight of the particle and the constraining effects of neighboring grains. A particle is subject to a drag or tractive force resulting in the difference in the fluid pressure on its upstream and downstream sides. Particles are also subject to a lift force occurring from the acceleration in the flow of water. This leads to a reduction in pressure above the grain and is known as the Bernoulli effect. Another type of bedload transport is saltation, where particles are moved along the channel bed at low angles, like short jumps. In addition, solid particles may experience irregular trajectories in suspended motion, which is more prolonged than saltation (Charlton, 2007; Summerfield, 1991).

Transportation of material in rivers could be either a dissolved load (solute), that is the result of intense bedrock erosion, or solid elements. Therefore, two types of load are defined: bed load and suspended load. Broadly, the difference is in the size of the particles, with the latter being so fine that are kept in suspension by upward momentum in turbulent flows. This two types of sediment are constant subject to abrasion and weathering (Summerfield, 1991).

3.4 Type of river channel

Rivers are complex systems influenced by multiple factors. Among these, sedimentation is probably the most prominent and the easiest to observe as directly influence the path and shape of the river. There are various type of river channel and they all have peculiar characteristics according to the surrounding environment.

By alluvial channels it is intended that the rivers that are formed by transported sediment by water flow. Since these type of rivers are prone to erosion, their form might considerably change as factors like discharge or sediment supply change. Hugget (2007) recognise four types of alluvial channels: straight, meandering, braided, and anastomosing. Charlton (2007) includes also anabranching channels in this category.

Straight channels are quite unusual to find, as it is generally limited to stretches of V-shaped valleys. Find this type of channel in flat areas normally means that is artificial, like many channels in the Netherlands. Moreover, also in straight channels the thalweg (the line of lowest elevation that marks the direction of the channel) twists from side to side (Hugget, 2007).

On the contrary, meandering channel type is probably the most known type of river channel and well defined in the collective imaginary. Erosion, undercutting, deposition and the formation of point bars are all provoked by the distinguished water flow pattern. This type of channel is highly dynamic compared to the straight channel and the position of the meanders tend to change, through cut-offs and avulsions (Charlton, 2007). This pattern is encouraged in landscapes where banks can resist the erosion. However, it is not fully understood why a river meanders.

Hugget (2007) suggests that this is attributable to the distribution and dissipation of energy within the river, a helical flow or an interplay of bank erosion. He also points out how the instabilities of turbulent water against a mutable bank might cause meandering.

Braided channels are characterized, according to an old definition given by Lane (1957), by "*having a number of alluvial channels with bars and islands between meeting and dividing again, and presenting from the air the intertwining effect of a braid*". This series of islands and bars are generated by accumulated sediment (Bristow & Best, 1993). While the latter are much more volatile, the islands tend to support vegetation growth, that will help to stabilize the sediments. Yet, a highly variable stream discharge, which alternatively brings degradation and aggradation to the channel, offsets this stabilization process. In literature ((Bristow & Best, 1993; Charlton, 2007; Hugget, 2007; Summerfield, 1991), it is well accepted that braided rivers tend to form where there are high rates of energy expenditures, the channel slope is steep, sediment supply is transported as bed load and bank material is erodible, letting the river path to move easily.

This type of channel is very common in alpine environments, where slope gradients are steep, and the river bed is composed of gravel. This is the case of the study area of the present research, as the Le Petit Buëch can be identified as river with a braided pattern. They also form in channels where there is high sediment load and the river bed is composed of sand and silt, as in parts of the Brahmaputra River. (Akhtar, Sharma, & Ojha, 2011).

Similar in the look to braided rivers anastomosing channels have a set of interconnected branches, separated by bedrock or by stable alluvium, that re-join, while braided rivers a single channel form. Their formation is backed up by an aggradational regime involving a high suspended-sediment load in sites where lateral expansion is constrained (Hugget, 2007).

Lastly, anabranching channels are rare to find and consist of two or more separated channels. In between the channels large islands are formed and often are well-vegetated. The development of anabranching channels usually flood frequently flood, channel banks that resist erosion, and mechanisms that block or restrict channels and trigger avulsions (Hugget, 2007). Differently from braided rivers, rates of lateral channel migration are usually quite low (Charlton, 2007).

3.5 The problem of bank erosion

Having a clearer vision on river processes and formation will help now to better understand the problem of bank erosion. As seen before, braided rivers like the Petit Buëch are subject to high levels of bank erosion. Due mainly to its morphology, Hautes-Alpes is one of the most sparsely populated regions of France. Soil loss, torrential

activity and hydric erosion are a common problem in all mountainous areas in the south of Europe (Descroix & Gautier, 2002) and this region is no exception to this problem. Downs & Simon (2001) noted how bank erosion can also have an impact on flood carrying capacity and not only channel morphology, as it affects the supply of sediment and large wood debris.

Seasonal precipitation and snow melt heavily influence the hydrological system, not only of this catchment, but of all the southern alpine region. Numerous floodplains show rivers with a braided pattern like the Buëch. Bravard, Landon, Peiry, & Piégay (1999) explain this as a cause of their proximity to coarse sediment sources and irregular hydrological conditions.

3.5.1 Reforestation influence

Hautes-Alpes knew a recolonization of the vegetation on the slopes. This reconquest is linked to the agro-pastoral abandonment of these areas but also and especially thanks to the reforestation and the successful correction of torrential watersheds by the Restoration of the Lands in Mountain (Restauration de Terrains en Montagne). These torrents were the main suppliers of sedimentary material, therefore, the quantities of sediments injected by the torrents into the three branches of the Buëch have certainly decreased significantly in the course of the 20th century due to the alleviation of erosive processes on the slopes (Gautier, 1994).

3.5.2 A multifaceted threat

The Petit Buëch showed, over the last five years, a constant change in its river bank form (Hemmelder et al., 2018), closing the gap with human settlements and roads, eroding agricultural land and posing a serious threat to the nearby train line.

According to the report by Barbero & Chappaz (2010), in the Buëch drainage area there are 362 farms present that share 32.418 ha of Useful Agricultural Area (UAA). Most of this UAA are pastures and forage areas, in fact 68% are dedicated mainly to livestock while 26% is dedicated to the production of arboreal.

However, there is a differentiation between the northern (that includes the study area, up to Serres) and southern area of the watershed. Indeed, in the northern part we find 54% of the total farms and most cattle farmers are found in this area, as well 46% of the sheep's farmers. This is due to type of agricultural surface present in the area, with 76% of the total rangelands and 72% of the fodder catchment areas.

Agriculture and fruit production are also present in the valley but with lower dominance. Orchards represent 18% of the total area in the watershed (about 179 ha), while 278 ha are dedicated to agricultural parcels (e.g. cereals, sunflowers, temporary crops).

As river bank erosion might have an impact on these agricultural catchments, on the other hand, it has to be considered the impact of this activities on the surrounding environment. Barbero & Chappaz (2010) identified the possible impact as an intensification of agricultural practices, by abandoning mowing/grazing practices on natural grasslands, leading to water withdrawals for agricultural irrigation and aggravating the already low water levels over summer.

The extraction of aggregates has been a common practice in the Buëch catchment area (Gautier, 1994), not only on the main branch but also on its tributaries, due to the good quality of the materials extracted. It is estimated that (Barbero & Chappaz, 2010), since the extractions started in the 1950s, 5.8 Mm^3 of material has been extracted in the entire watershed. Comparing this to the annual solid volume carried by the river, which is estimated at 60000 m^3/year, gives a good viewing on the intensity and the potential impact on river dynamics. This impact is reflected in a local incision of the bed, but also by regressive and progressive erosions that implicate a lowering of the river bed. The alluvial samples also generate a sediment deficit in the downstream sections, resulting in disturbances to dynamics of the watercourse (Bravard et al., 1999).

The management of rivers is of great importance because bank erosion, quite problematic in braided rivers, can deal a lot of issues. Soil loss, that could be translated in numerous problems, with a great damage to natural

resources and human infrastructure. Therefore, it is not a hard to guess why bank erosion is considered not only a major problem in river management but an actual natural hazard that must be limited (Piégay, Darby, Mosselman, & Surian, 2005).

Controlling rivers, not only their intrinsic characteristics such as water quality or more physical aspects such as mass flow rate and temperature, is a key aspect in water management in all countries at all governmental levels. Moreover, in the case of braided and meandering rivers, the attention given from administration is and should be higher due to their volatile and dynamic nature (Piégay, Grant, Nakamura, & Trustrum, 2006).

4 Study Area

This study will tackle a similar problem already researched in the past (Hemmelder et al., 2018) and will continue its work, however, the constant changing of the shape and location of the river bank give the possibility to renew the study proposition and further analyse, thanks to GIS tools and technologies, by extending the existing time series of drone images and shed more insight what are the critical issues and where they are located. The study areas chosen are two and are both located on the Petit Buëch river path, at Pont du Chabestan and at La Bâtie-Montsaléon **(Figure 1 and 2)**

Figure 1 *Study area at Le Pont Chabestan, 2013 (source IGN)*

Figure 2 *Study area near La Bâtie-Montsaléon, 2013 (source IGN)*

4.1 Hydrology

The Petit Buëch river is a tributary of the Buëch which is, in turn, a tributary of the Rhone by the river Durance. Its spring is located under the Pic de l'Aigulle and surrounded by Dévoluy and Bochaîne massifs, which strongly influence the regimes of the Petit Buëch (SDAGE, 2013) **(Figure 3)**

The hydrological behaviour of the Buëch watershed is highly affected by seasonal variations: sudden and, sometimes, violent flood in autumn/winter season and very low water levels in summer. The hydrological regime is therefore twofold: the river is "alpine" from January to June and "Mediterranean" from July to December. The hydrological regime of the watercourse is undoubtedly influenced by withdrawals, mainly agricultural, and regulated flow downstream of the Saint-Sauveur dam (Barbero & Chappaz, 2010).

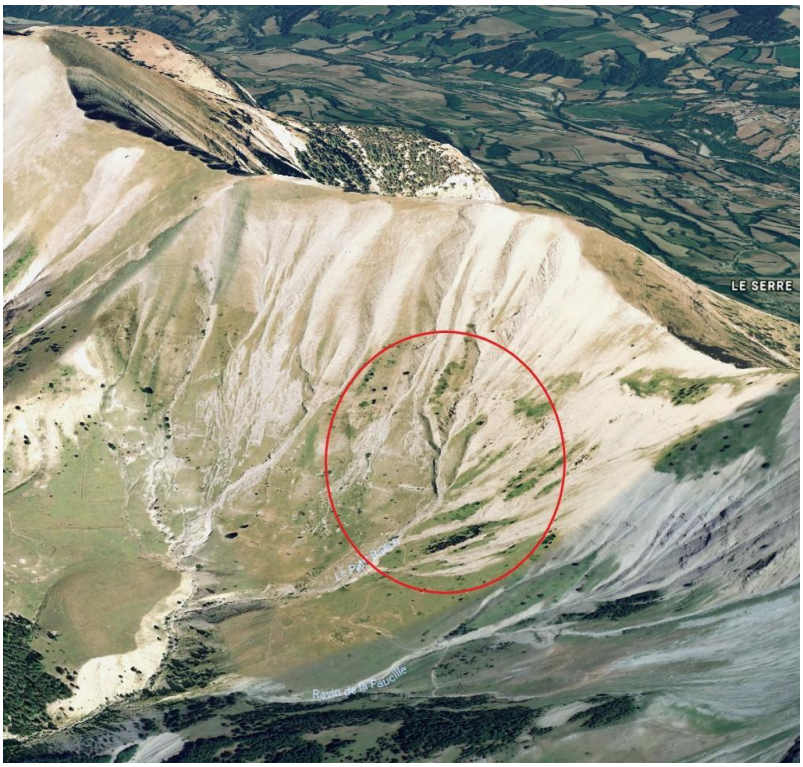

Figure 3 *Petit Buëch spring source, 2018 (source Google Earth)*

4.1.1 Discharge

The availability of discharge data on the Petit Buëch is scarce and inconsistent. However, some data can still be retrieved on the HYDRO website page of the French Ministry of Ecology, Sustainable Development and Energy. Down in the table below are shown some data retrieved from the Laragne discharge station, on the main branch of Buëch river after the confluence of Petit Buëch and Grand Buëch at Serres.

Table 1 *Data on Buëch (SDAGE, 2013) and (Brocard & Beek, 2006).*

Basin Surface (Km^2)	Longest Hydraulic Path (Km)	Max Altitude (m)	Min Altitude (m)	Mean Annual Discharge ($m^3 s^{-1}$) *	Peak Discharge ($m^3 s^{-1}$) *	Maximum Measured Peak Discharge ($m^3 s^{-1}$) *
388.1	44.25	2650	650	16	370	557

**These values where recorded at Laragne discharge station*

4.2 Climate

The Mediterranean climate of the area is clearly influencing its hydrogeological regime, with the heaviest rainfalls during autumn and spring, and a mean annual rainfall of approximately 800 mm. Moreover, moderate spring snowmelt further influences its regime (Irstea & Conseil Départemental des Hautes-Alpes, 2017).

The following tables and graphs show the monthly variations in temperature and precipitation registered at the weather station in Gap, about 35 Km from the study area and the closest one. However, it must be pointed out how the precipitation data are incomplete. Both years present a month without data (December 2016 and October 2017), while January 2017 shows unusual low values. The data were found on infoclimat.fr

Table 2 *Temperature at Laragne-Monteglin weather station, 1992-2010*

	January	February	March	April	May	June	July	August	September	October	November	December	Whole Year
Maximum temperature (average in °C)	7.3	10.5	15.2	17.8	22.9	27.7	30.4	29.7	24	18.9	11.8	7	18.6
Average temperature (average in °C)	2.1	4.2	8.1	10.8	15.5	19.6	22	21.5	16.8	12.5	6.5	2.4	11.9
Minimum temperature (average in °C)	3	-2.1	1	3.9	8.2	11.5	13.6	13.3	9.5	6.2	1.2	-2.1	5.1
Average Days Max Temperature ≥ 30°	.	.	.	0.1	1.4	10.4	19.1	15.4	2.2	.	.	.	48.6
Average Days Max Temperature ≥ 25°	.	.	0.3	1.4	10.3	21.7	28.2	27.3	13.1	1.6	.	.	103.9
Average Days Max Temperature ≤ 0°	0.7	0.2	.	.	.	.	.	.	.	.	.	0.6	1.5
Average Days Min Temperature ≤ 0°	22.8	20.3	13.3	3.1	0.1	.	.	.	.	1.6	13	20.7	94.9
Average Days Min Temperature ≤ -5°	10.7	6.4	1.4	.	.	.	.	.	.	.	2.2	7.8	28.5
Average Days Min Temperature ≤ -10°	1.7	0.8	0.1	.	.	.	.	.	.	.	0.2	1.1	4

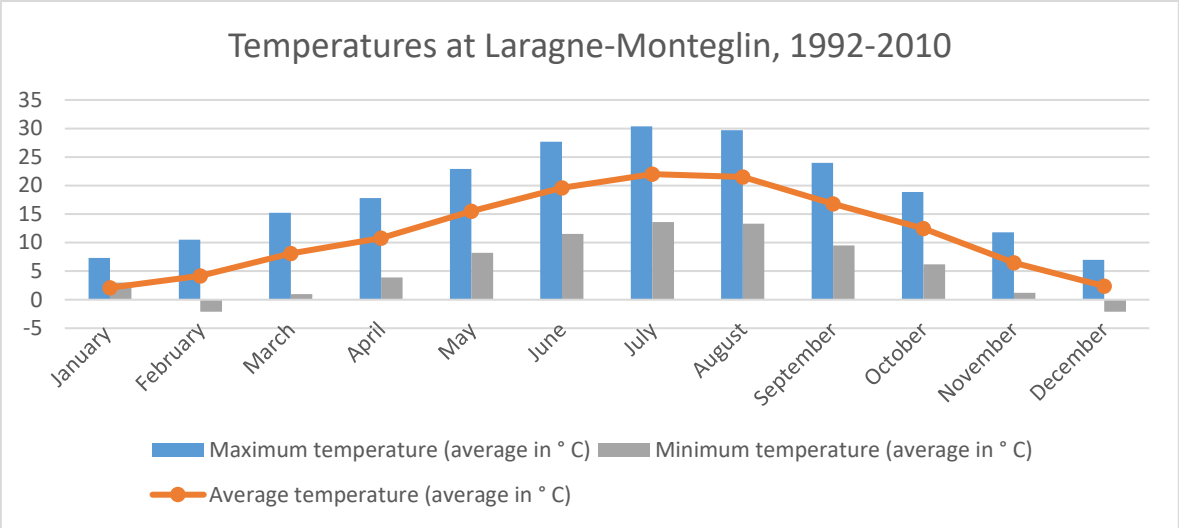

Figure 4 *Graphical representation of Min-Max and Average temperatures at Laragne-Monteglin weather station*

Table 3 *Precipitation at Laragne-Monteglin weather station, 1992-2010*

	January	February	March	April	May	June	July	August	September	October	November	December	Whole Year
Maximum Daily Rainfall Height (mm)	109.5	52.5	41	75.1	53.5	91.4	54.3	65.8	78.5	86.6	118.3	58.7	118.3
Average Precipitation Height (mm)	68.6	40.6	36	79.7	73.5	53	37.4	50.4	98.1	99.6	107	71.3	815.2
Average Number of Days with Height ≥ 1 mm	6.7	4.8	5.3	8.3	8.6	5.5	4.4	5.6	6.6	7.6	8.3	7.7	79.5
Average Number of Days with Height ≥ 5 mm	3.8	2.4	2.4	4.5	4.6	3	2.3	2.8	4.4	4.7	4.8	3.8	43.7
Average Number of Days with Height ≥ 10 mm	1.9	1.5	0.8	2.8	2.5	1.6	1.2	1.8	3	3.2	3.1	2.4	25.9

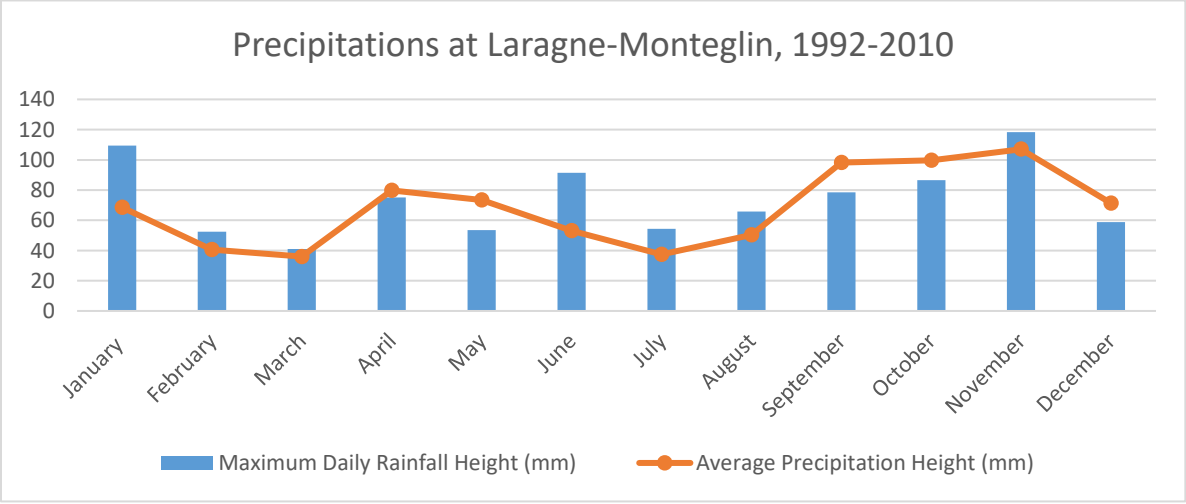

Figure 5 *Graphical representation of Maximum and Average precipitation heights at Laragne-Monteglin weather station*

4.3 Topography

4.3.1 Geology

The geology of the river Buëch area is constituted by a thick sedimentary cover, from Jurassic and Cretaceous ages, of interbedded marls and limestones (Brocard, van der Beek, Bourlès, Siame, & Mugnier, 2003) to compose the majority of the lithology, as usually found in this area. Moreover, the Petit Buëch branch shows marginal glacial deposits form the Last Glacial Maximum (LGM). Yet, in the subcachements draining the Dévoluy Massif a large quantity of loose superficial debris, belonging to Cretaceous limestones that cracked up due to frost are present and accumulated in large talus slope deposit (Irstea & Conseil Départemental des Hautes-Alpes, 2017).

The various branches of Buëch present accompanying layers that circulate in alluviums of greater or lesser thickness. Their extension is limited by the presence of black marl forming an impermeable substratum. The plain of Petit Buëch is made up of 3 successive basins: the basin of Roche des Arnauds - Devès, the basin of Montmaur and the valley of Veynes at Pont la Barque. The alluvial plain of Buëch, between Serres and Sisteron, forms a succession of basins alluvial deposits separated by rocky cracks. The tablecloth is therefore discontinuous. The underground resource available on the Buëch watershed remains unknown (Barbero & Chappaz, 2010).

4.3.2 Land Use and Land Cover

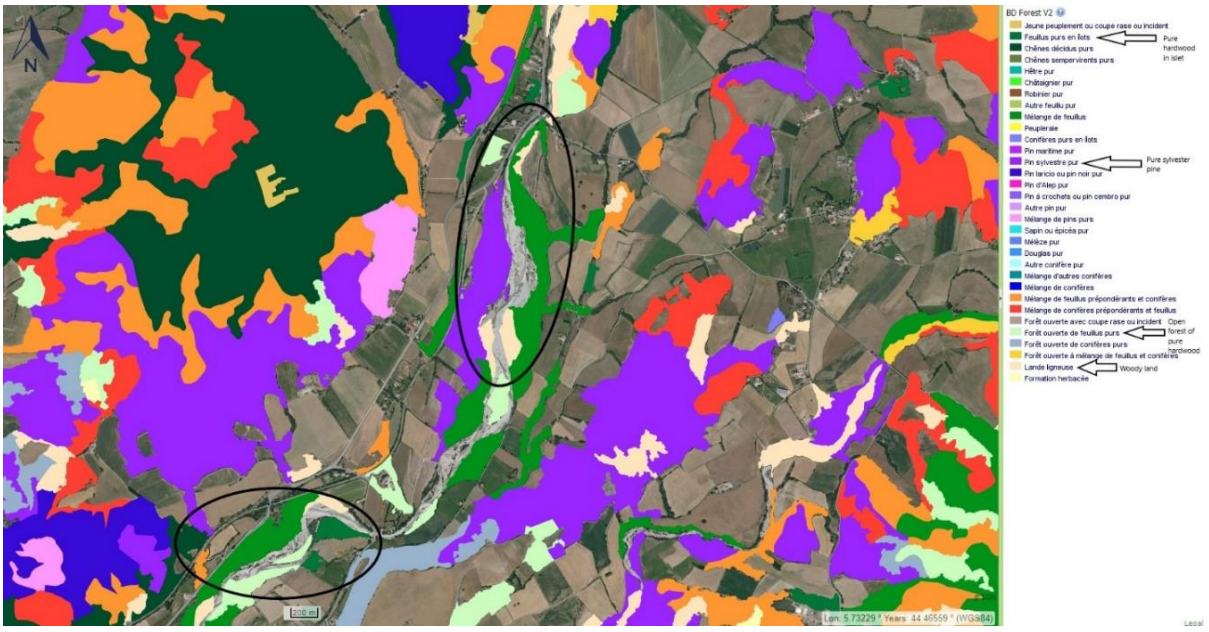

Figure 6 *Forestry land cover in the study area*

In 2010 the Hautes-Alpes department had 135 kha of tree cover, extending over 24% of the land area. In 2017, it lost 367ha of tree cover (Global Forest Watch, date). The types of forest covering the study area are: islets pure hardwoods (the relative free cover rate of hardwoods, excluding poplars grown, is ≥ 75% and they correspond to isolated stands that cannot be attached to one more forest big surface), open forest of pure hardwood (the relative free cover rate of pure hardwood is ≥ 75%. It is the grouping of all broadleaved species), pure Sylvester pine and woody land (the vegetation that constitutes it is a spontaneous vegetation which includes a significant proportion of woody plants (heather, broom, gorse, various spiny) and semi-woody (ferns, phragmites...) whose height does not exceed 5 meters. (IGN, 2016).

géoportail

Corine 2012 Land Use Map

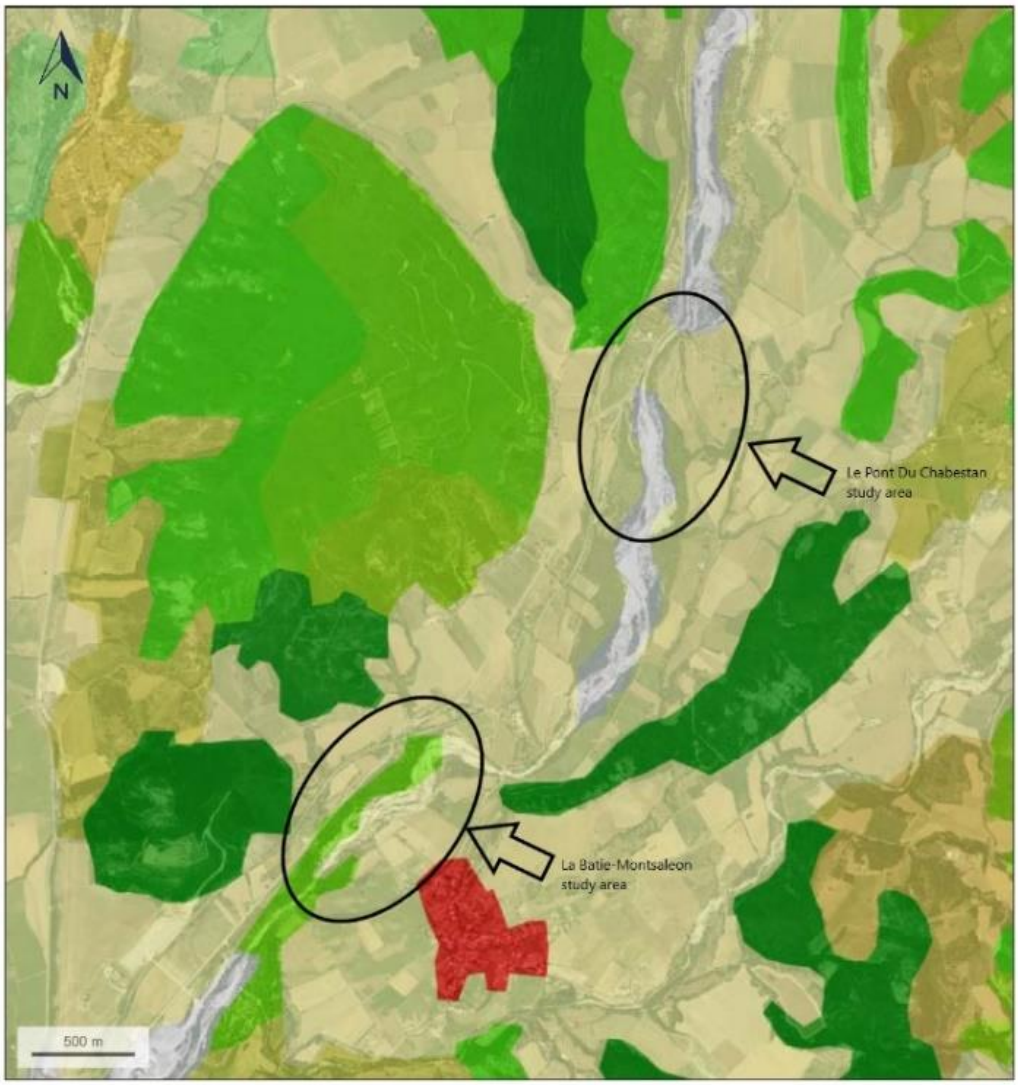

Longitude : 5° 45' 14" E
Latitude : 44° 28' 24" N

Corine land use map of the study area, at La Bâtie-Montsaléon and Le Pont Du Chabestan. - In red: Discontinuous urban fabric - In light green, in the river area: Hardwood forests - In light yellow: Arable land outside irrigation perimeters - In light gray: Beaches, dunes and sand - In dark green: Coniferous forests

Figure 7 *Corine Land Use map of the study areas*

5 UAV photogrammetry

The start of photogrammetry can be dated back to 1849 with the work of Aimé Laussedat and the start of table photogrammetry. Yet, photogrammetric techniques were mainly applied for mapping purposes and military espionage. The reason behind this narrow field development is to ascribe to the poor results obtained despite the huge resources required to achieve them. Photogrammetry has to wait till the '60s of XX century to see a broadened use of its techniques, for topographical surveys and the start of annual gathering of aerial data (The Center for Photogrammetric Training, n.d.). However, the "golden age" of photogrammetry started in the mid '90's with the digitization of the data and digital acquisition of the aerial imagery. This led, in the last 20 years, to a fast development of photogrammetric techniques, increasing the quality of data obtained while enormously reducing the costs. In this context, the use of Unmanned Airborne Vehicles (UAVs) is the natural evolution of 150 years of aerial photography.

Nowadays, UAV imagery is used for multiple purposes that include:

- Environmental surveying, such as:
    - Soil erosion (Pineux et al., 2017);
    - River bank (Dietrich, 2016; Fonstad, Dietrich, Courville, Jensen, & Carbonneau, 2013; Javernick, Brasington, & Caruso, 2014) and, in general, water monitoring;
    - Forestry and agriculture (Grenzdörffer, Engel, & Teichert, 2008), for rapid and low cost assessment of crops state, forest surveillance, recognition of types of plants and areas favourable to silviculture;
- Archaeology, for surveillance of sites which have limited accessibility (Aicardi et al., 2016) and 3D reconstruction and monitoring of these sites (Gonizzi Barsanti, Remondino, & Visintini, 2013);
- Emergency response (Aicardi et al., 2016; Haarbrink & Koers, 2006) and rapid assessment tool in flooding events (Smith, Carrivick, Hooke, & Kirkby, 2014);
- Cost-effective 3D reconstruction of man-made structures (Aicardi et al., 2016; Gonizzi Barsanti et al., 2013; Irschara & Kaufmann, 2010) and natural landscapes (Diaz-Varela, Zarco-Tejada, Angileri, & Loudjani, 2014).

5.1 Advantages

The advantages brought by the use of UAVs in photogrammetry are testified and proven by multiple studies over the last 20 years. Remondino & Barazzetti (2012) point out how UAVs can produce high quality products in situations where rapid assessment of critical situations is required. This allows to have near-real time data, which is of pivotal importance in emergency response as well as for classic field survey. Moreover, they also highlight that using rotatory wing UAVs as the advantage of vertical take-off and landing, allowing its use in nearly every environment.

Looking specifically in the literature regarding remote sensing of rivers, Dietrich also emphasizes how the recent introduction of the SfM (Structure-From-Motion) algorithm has pushed the use of UAVs in photogrammetry projects, giving new and cheaper opportunities to researchers. SfM doesn't require professional and expensive cameras to capture the imagery. As a matter of fact, the camera used in the flights is a compact high-resolution digital camera designed for underwater usage. Moreover, SfM requires a lower number of Ground Control Points (GCPs) (Javernick et al., 2014; Westoby, Brasington, Glasser, Hambrey, & Reynolds, 2012), speeding up the processing of the data. The use of multiple cameras views, from different angles, enhance the precision of the obtained point cloud products. This point cloud is then converted into a 3D model and/or a DEM, while the imagery can be mosaicked and rectified to the DEM. The results obtained by Dietrich (2016) show how the SfM workflow is proven to have cost-effective efficiency for large scale river catchments.

One of the advantages of using SfM and UAVs in photogrammetry, as said in the previous paragraph, is the possibility to capture the photographs from different angles (even upside-down) and use it without any pre-processing need. The use of oblique imagery in photogrammetry is proven in different research (Aicardi et al., 2016; Hemmelder et al., 2018). Aicardi et al. (2016) underline that this technique is well suited for Cultural Heritage surveillance and study, but also well applies to emergency response. This also allows to take photos less "accurate", that is not necessarily parallel to the ground, but requires more thoughts to put into the route

planning in order to have a perfect overlap between each photograph. Kršák et al. (2016) also highlight that, if well equipped, UAVs can register some vital flight data such as flight altitude and camera coordinates, setting up automatically the exterior orientation parameters of each photo.

Lastly, is worth to remember that the use of UAVs can be easily integrated with other photogrammetric techniques (e.g. Terrestrial Laser Scanning or TLS), to enhance the quality of the data obtained (Remondino & Barazzetti, 2012).

5.2 Disadvantages

UAV photogrammetry and the SfM workflow certainly have advantages but also have shown some flaws. As said this methodology can be applied also by using non-professional cameras however, this impose to acquire a larger number of photos to achieve the same coverage at a similar resolution (Remondino & Barazzetti, 2012). They also highlight other external contingencies that may affect the use of UAVs for photogrammetric research: in windy areas low-cost UAVs are not well suited for the task and research at high altitudes (on glaciers perhaps) might influence the mechanical performance of the UAV itself. Another drawback he points out is the fact that multiple personnel may be required to carry and control the vehicle.

By controlling the UAV, it is not intended purely its direct control. If not equipped with tracking sensors, it's hard to judge UAV's height, its speed and the range distance from the operator. These might bring to different problems in the data acquisition: perceived coverage differs from actual coverage, insufficient overlap of photographs, multiple flights needed if the area is larger than the control range of the UAV (Cook, 2017).

Gonizzi Barsanti et al. (2013) point out how the modelling part, from point cloud to 3D model, is still the most problematic due to the high time consumed to obtain a satisfying product. However, this is a problematic related to the need of a high-end computer to quickly process the data more than an actual drawback in the workflow. Yet, he also stresses out how the major drawbacks are related to external factors and operator experience. He compares photogrammetry to laser scanning techniques noticing that, while the latter have harder to process data, they also are easier to use in surveying. This because photogrammetry needs to be accurate in the gathering of the imagery and an eventual lack of good positioning reference would greatly hinder the quality of the model (Cook, 2017). Yet, both techniques can deliver ultra-high-quality resolution and accuracy products if the surveying phase is well-planned (Gonizzi Barsanti et al., 2013).

5.3 Improvements

The given advantages and disadvantages provide room for a small excursus on the possible improvements to UAV photogrammetry techniques. The use of DGPS (like in this research) will be more common and cheaper over the next years, while the constant enhancement of computer technology might lead this kind of research to be almost exclusively on the field, with nearly no post-processing work to do in labs (Remondino & Barazzetti, 2012).

Furthermore, the planning of the flight has room for improvement. Remondino & Barazzetti (2012) suggest developing a tool for simplifying this task. A "blueprint" for automate flights according to the area and the environmental condition could be another solution.

Lastly, unrelated to the strict technical side, Remondino & Barazzetti (2012) also highlight the need for more technical specification and regulations over UAV survey, setting boundaries on where and when they can be used, avoiding invasion of privacy and establishing precisely the range of their application.

6 Methodology

In this section the dataset used, the data processing workflow, the software and hardware used in this study will be outlined.

6.1 Dataset

The dataset used in this study is a collection of images acquired by an Unmanned Airborne Vehicle (UAV) operated by Henk Markies. To the author, Utrecht University made available two datasets: one from 2016 and another from 2017. Both datasets are raw and need to be processed. Yet, other than the raw photographs were also provided to the author a Microsoft Excel file with the location of the DGPS.

Table 4 *Number of photos per flight for each dataset*

Location	2016							2017			
La Batie - Montsaléon	1	2	3	4	5	6		1	2	3	4
	88	67	28	43	77	46		188	130	249	327
Total	349							894			
Pont Chabestan	1	2	3	4	5	6	7	1	2	3	
	115	148	166	67	175	231	200	89	146	205	
Total	1102							440			

The photos where all taken in June between the 9th and 12th, both in 2016 and 2017. Moreover, the camera used is the same as the format type **(Table 5)**. The camera used is the same as for previous works in the same area (Hemmelder et al., 2018), therefore this should facilitate the data processing workflow and the comparison of the results.

Table 5 *Camera details*

Dataset	Camera Model	Resolution (Width x Height) (in pixels)	Focal Length (mm)	Type
2016 - 2017	Canon PowerShot D10	4000 x 3000	6	JPEG

6.2 Software

The software that will be used to process the imagery will be Agisoft PhotoScan Professional. It is an advanced 3D modelling software, which can create high quality 3D content from still imagery. It operates with arbitrary images in both controlled and uncontrolled conditions, with pictures taken from any position and angle (Agisoft, 2018). Yet, the object must be visible I at least to images to let the program work successfully. Lastly, both the alignment and 3D model reconstruction are fully automated, using the Structure-from-Motion algorithm (Smith, Carrivick, & Quincey, 2015).

As pointed out by its manual (Agisoft, 2018), the procedure of 3D reconstruction involves four main steps:

1. Camera alignment: the program looks for common points in the imagery and matches them. Moreover, it locates the position of the camera for each picture and refine its calibration parameters. The result is a sparse point cloud and a set of camera positions are formed.

2. Building a dense point cloud: Based on the previous stage results the program builds a dense point cloud. The resulting point cloud could be edited and classified prior the next step.

3. Building a mesh: the program reconstructs a 3D polygonal mesh of the object/area surface. PhotoScan give a choice between two algorithmic methods for the 3D mesh creation: *Height Field* – for planar surfaces, *Arbitrary* – for any kind of object.

4. Texturing and/or OrthoMosaic generation.

PhotoScan by Agisoft is the main software that has been used for the processing steps of this research. After all the dataset are processed, the outputs yielded will be analysed in other programmes that are better suited to work with geographic data like ArcMap and ArcGIS Pro, while for any graphical correction of the OrthoMosaics Adobe Photoshop might be of use.

6.3 Data processing workflow

The author decided to follow the general workflow proposed in the PhotoScan manual (Agisoft, 2018). This is due to the lack of knowledge and experience with the program. Nevertheless, this workflow has been widely used in similar research (Hemmelder et al., 2018; Smith et al., 2014, 2015) and is proven to deliver the expected output.

1. **Loading photos into PhotoScan**: The imagery is loaded in the programme. I first quality check is made beforehand, in order to eliminate clearly blurred or non-useful images (e.g. before take-off).

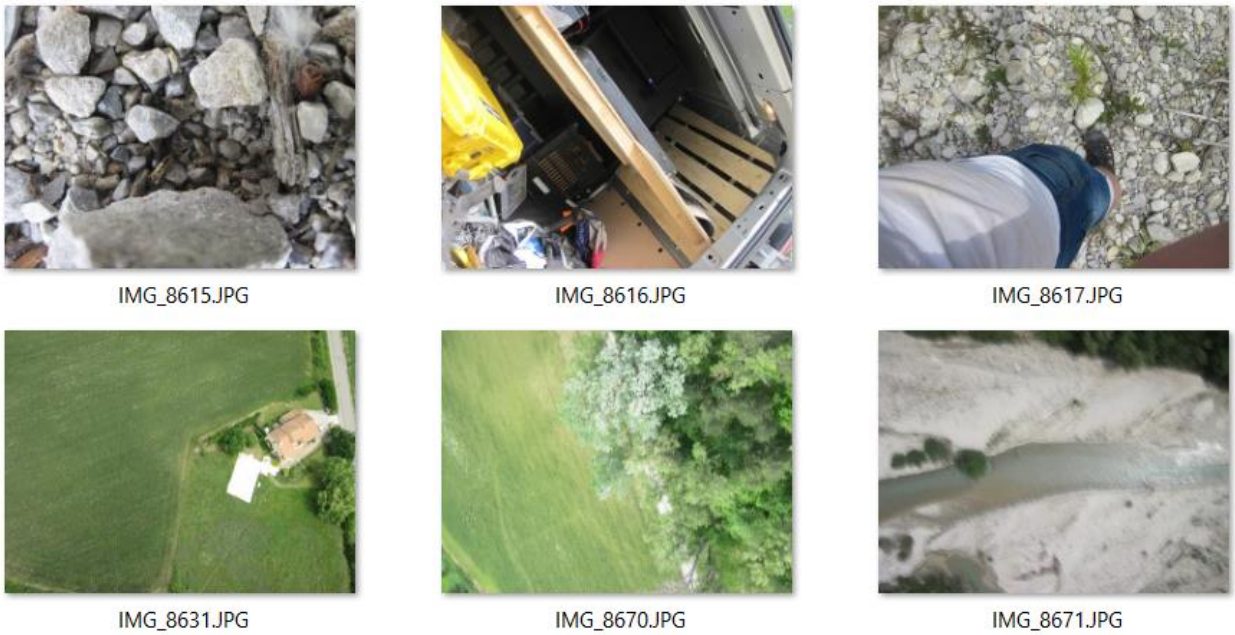

Figure 8 *An example of the imagery dataset*

2. **Inspecting loaded images**: The imagery quality is inspected a second time with a tool that will give the user an estimation of the quality of each image with a number ranging from 0 to 1. Usually it is suggested to discard all of the imagery that rate below 0.5, but it is always better to double check again these images as sometimes the programme tend to rate some imagery with unrealistic ratings. This tool is mainly useful to be sure the user doesn't miss any clear unusable imagery that managed to pass through the first sorting.

Label	Size	Aligned	Quality	Date & time	Make	Model	Focal length	F-stop	ISO	Shutter
IMG_3144	4000x3000	✓	0.796012	2017:06:10 15:1...	Canon	Canon PowerSh...	6.2	F/2.8	80	1/1250
IMG_3143	4000x3000	✓	0.697647	2017:06:10 15:1...	Canon	Canon PowerSh...	6.2	F/8	80	1/200
IMG_3142	4000x3000	✓	0.775059	2017:06:10 15:1...	Canon	Canon PowerSh...	6.2	F/2.8	100	1/1000
IMG_3141	4000x3000	✓	0.724209	2017:06:10 15:1...	Canon	Canon PowerSh...	6.2	F/2.8	80	1/1250
IMG_3140	4000x3000	✓	0.80492	2017:06:10 15:1...	Canon	Canon PowerSh...	6.2	F/2.8	80	1/500
IMG_3139	4000x3000	✓	0.687638	2017:06:10 15:1...	Canon	Canon PowerSh...	6.2	F/8	80	1/250
IMG_3138	4000x3000	✓	0.775573	2017:06:10 15:1...	Canon	Canon PowerSh...	6.2	F/2.8	160	1/800
IMG_3137	4000x3000	✓	0.795939	2017:06:10 15:1...	Canon	Canon PowerSh...	6.2	F/2.8	125	1/500
IMG_3136	4000x3000	✓	0.804224	2017:06:10 15:1...	Canon	Canon PowerSh...	6.2	F/2.8	100	1/500
IMG_3135	4000x3000	✓	0.804864	2017:06:10 15:1...	Canon	Canon PowerSh...	6.2	F/2.8	80	1/1250
IMG_3134	4000x3000	✓	0.790262	2017:06:10 15:1...	Canon	Canon PowerSh...	6.2	F/2.8	80	1/1250
IMG_3133	4000x3000	✓	0.579002	2017:06:10 15:1...	Canon	Canon PowerSh...	6.2	F/8	80	1/320
IMG_3132	4000x3000	✓	0.744062	2017:06:10 15:1...	Canon	Canon PowerSh...	6.2	F/2.8	100	1/1250
IMG_3131	4000x3000	✓	0.648345	2017:06:10 15:1...	Canon	Canon PowerSh...	6.2	F/8	80	1/250
IMG_3130	4000x3000	✓	0.789112	2017:06:10 15:1...	Canon	Canon PowerSh...	6.2	F/2.8	160	1/1000

Figure 9 *The "photo pane" view in PhotoScan*

3. **Aligning photos**: At this stage, the Structure-from-Motion algorithm scan each photo and assign common points to each one of them: The programme then aligns all the photos together and create an unreferenced sparse point cloud. After this first output the user, if in possession of any reference, starts to assign various Ground Control Points (GCPs) to georeference it. In the case of this research, the georeferenced came in a CSV file that could be imported in the programme. Once the reference is imported, the programme will create DPGS markers that needs to be assigned to the respective marker in the photos. This step could be very time consuming as in some cases markers can be assigned up to 80 photos. However, the programme is quite good in auto-assign the DPGS coordinate to right marker after a couple of them are positioned manually. Clearly, the more coordinates assigned manually the least error is expected. Yet, this is not always the case, as some photos will have a high error (in the case of this research, over 15 cm) because of the poor quality of the photo or the low number of photos where the marker is visible.

   After the point cloud is georeferenced, good practice is to optimize the alignment at least a second time to further reduce the positional error and yielding a higher quality point cloud. Besides, at this stage the programme allows to select some points according to their projection error and uncertainty reconstruction, allowing the user to "trim" the point cloud and clean it from most of the noise that could be created (e.g. reduced "jumping fish" effect from the water areas of the photos).

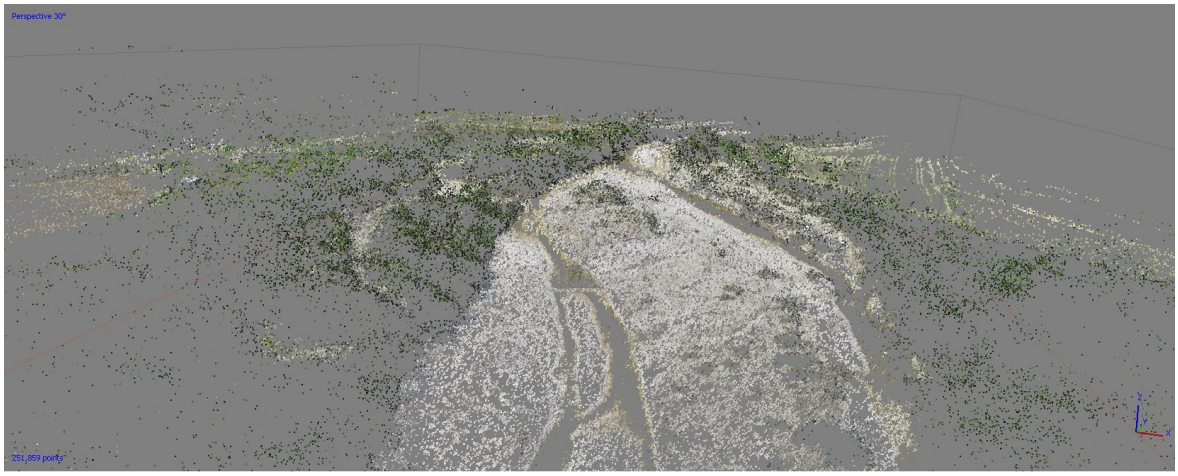

Figure 10 *The sparse point cloud*

4. **Building dense point cloud**: This step is already quite self-explanatory, as from the sparse point cloud the programme will build a much denser and thicker point cloud. This point cloud could also be the last step of the process, since to extract the DEM and subsequently the OrthoMosaic this what the user need. In fact, it is suggested on the PhotoScan manual to extract the DEM from the point cloud as it is more accurate then extracting it from the 3D mesh.

   Lastly, it is good to remind that this step is possibly the most time-consuming of all for computer processing. Working on one computer to obtain ultra-high-quality point clouds might take up to 4/5 days just to calculate the depth maps and another week of non-stop work to build the point cloud. The only way to speed up the process and maintain the same quality is to network multiple computers and share the processing power in a cluster. This way the improvement in processing time is huge, about 1 day and half to complete the whole process. A good reminder is that network processing can be set up for each of previous and following steps too, speeding up the whole process of about two weeks to create an ultra-high-quality 3D model (and relative DEM and OrthoMosaic) to just a couple of days of processing. Also, important to remind that network processing is sometimes mandatory if the user wants a ultra-high quality result, as sometimes even the computers of the GIS lab can't handle only by themselves all the processing, giving back "bad allocation" error because of not enough RAM available, shutting down the process sometimes even halfway through it.

Figure 11 *The dense point cloud*

5. **Building 3D mesh**: After the dense point cloud is built, the next step in the workflow is the TIN interpolation of those points and the creation of a non-textured 3D model. The result is a simple polygonal 3D model of the area. Since there aren't textures the model looks quite low quality, especially where the vegetation resides. The program allows to decimate the faces created with a specific tool and it is suggested to use it in order to reduce them, as PhotoScan tend to over-create polygons, increasing the size of the file and slowing down the next steps in the workflow.

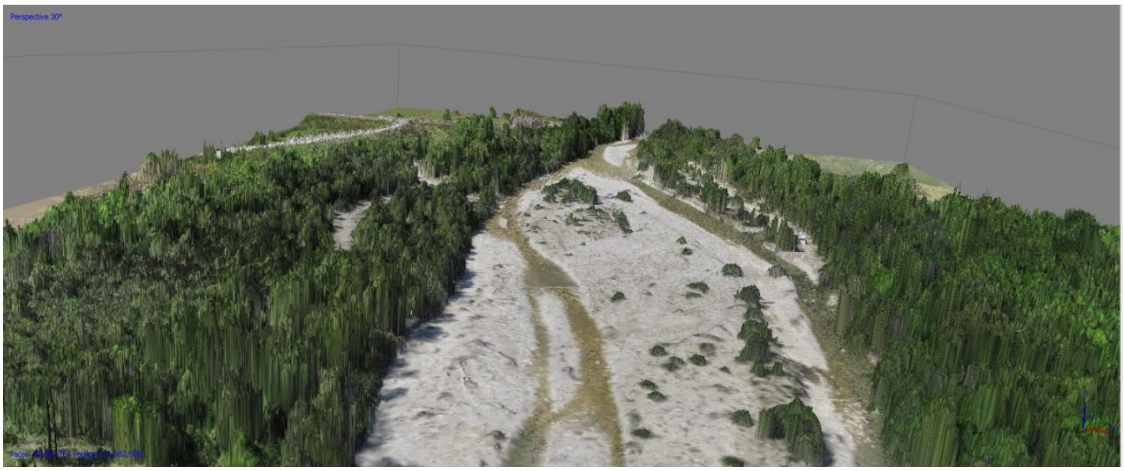

Figure 12 *The untextured 3D model*

6. **Generating texture**: The programme simply applies a texture to the 3D mesh, using the imagery available to texture the model.

Figure 13 *The textured 3D model*

7. **Building DEM**: This step could be anticipated, as said before, but building the DEM before or after the 3D model is done is up to the user and the time constraints he has. Extracting it from the dense point cloud will yield a more accurate product but doing this from the mesh will be slightly faster. The result will be a DSM of the whole catchment.

8. **Building OrthoMosaic**: The OrthoMosaic can be build using the DEM as source. This is possibly the best and fastest way to build it, since the extent is already defined, the two products will have a similar resolution. The result will be a georeferenced mosaic of all the photos loaded in PhotoScan. The final quality of the OrthoMosaic depends on multiple factors such as quality of the imagery, number of photos available, overlap between the photos and flight plan.

9. **Exporting results**: The resulting DEM and OrthoMosaic can be finally exported for further analysis. The program allows to export also all the other products yielded during the whole workflow, such as the point clouds and the 3D mesh.

As follows, also a graphical flowchart (**Figure 14**) that shows all the steps previously mentioned.

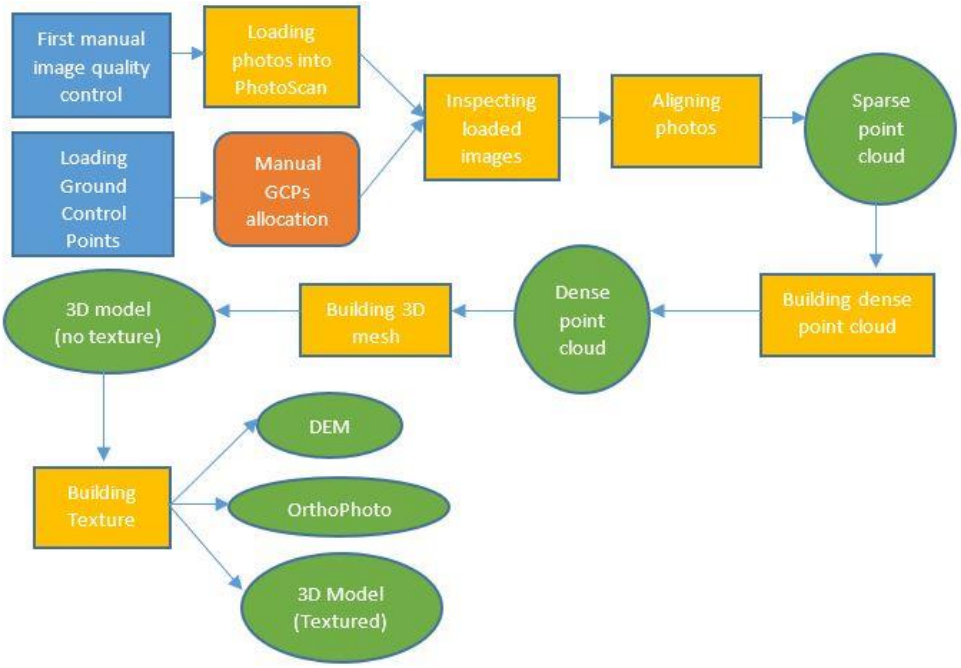

Figure 14 *PhotoScan workflow with the specific settings used for each step*

6.4 Hardware

The hardware that will be used during this study are shown in **Table 6** (see appendix). Utrecht University provided the author various computers available in the GIS labs, located at De Uithof, that will be mainly used to process the data. Even though the personal laptop could handle Agisoft PhotoScan, the main processing work will be done on these computers, as it is possible to run multiple process at the same time. Yet, the author will be using his personal laptop, as it is powerful enough to run minor processes on Agisoft with no trouble and can easily handle other software (e.g. ArcMap) that will be used for the analysis part.

Table 6 *Hardware specifications*

Computer	Manufacturer	System	Processor	RAM	Graphic Card
Utrecht University	HP	Windows 10 Enterprise 64-bit	Intel® Xeon® CPU E3-1245 v5 @ 3.50GHz (8CPUs)	32 GB	NVIDIA Quadro M620 18GB
Personal Laptop	HP	Windows 10 Home 64-bit	Intel® Core™ i7-7700HQ CPU @ 2.80GHz (8CPUs)	16 GB	Intel® HD Graphics 630 8 GB NVIDIA GeForce GTX 1050 8 GB

7 River Bank Analysis

In this section the methodology will be outlined describing how the analysis on the riverbanks will be carried out. The three outputs obtained from the previous workflow will be analysed from both qualitative and quantitative perspectives. The products obtained shall be of such high quality that a visual - comparative analysis of the OrthoMosaic might be already enough to assess the behaviour of the river over the last two years. Subsequent, quantifying the bank erosion and volume loss will answer and give further insight on the river dynamics.

7.1 Analysing channel path displacement

As seen in the introduction, the Buëch river is subject to erosion processes that, yearly, wear down its banks and therefore displace the channel path. The georeferenced OrthoMosaics can be superimposed with extracted river path shapefiles and the resulting image will show the two paths in two different colours (**Figure 15**), for 2016 and 2017 respectively, allowing a clear analysis of the change over the year.

The path could not be automatically extracted, also with the use of graphical programs such as Adobe Photoshop and Paint 3D. Therefore, the chosen solution was to simply manually digitize the path in ArcMap and create a new polygon shapefile out of the raster dataset. The main drawback of this solution is the lower accuracy of the analysis, but at the same time this ease the visual comparison of the different datasets over time.

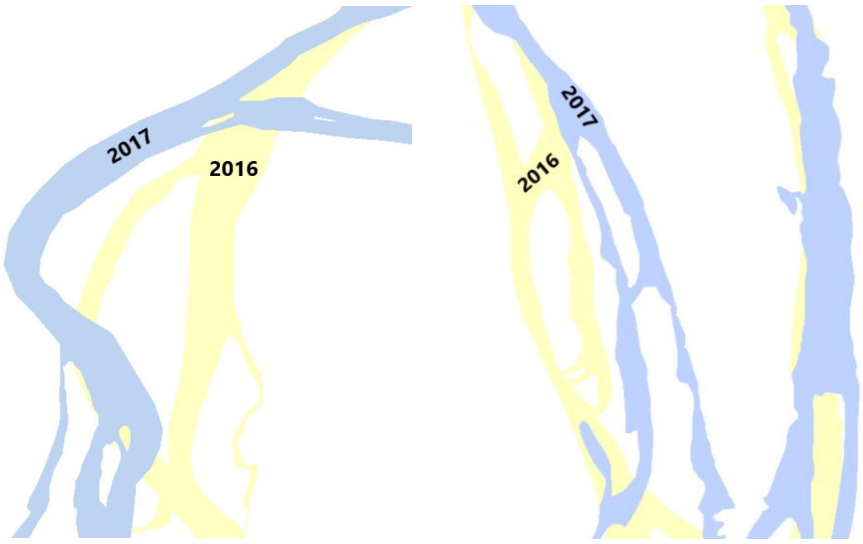

Figure 15 *River path at La Bâtie-Montsaléon (left) and Chabestan (right)*

7.2 Quantifying bank erosion

It is estimated by using the data extracted with the DEM. Smaller subcachements will be taken for the analysis by comparing the two OrthoMosaic. Transects will be “drawn” on the two OrthoMosaic and the cell values will be plotted in in a graph showing the transection as seen from ground level.

Agisoft PhotoScan has some tools useful for this purpose. The program, in fact, allows the user to carry out a first simple analysis just by drawing polylines in given areas and study their heights and profiles. Moreover, these polylines can be exported as shapefile and loaded in another PhotoScan project (perhaps the following year model), easing the comparison between years and avoiding inconsistencies between the compared areas over the years.

Other than PhotoScan, further analysis on the effect of the erosion of the river on the surrounding area can be studied using slope maps. These maps are obtained by extracting the slope gradient of the exported PhotoScan DEM in ArcGIS. Here, a much more suitable environment for DEM analysis, the DEMs from 2016 and 2017 are processed with the raster calculator and the result is a new dataset showing the difference in slope between 2016 and 2017.

7.3 Quantifying volume change

Two methods were used to estimate the volume change of the two catchments. At first, it was thought to follow the same methodology applied by Hemmelder et al. (2018), having a common method that would ease the comparison between years and give reliability to the results. However, the volume change analysis they carried out turned out to evaluate only a small sample in the area of La Batie-Montsaléon, limiting the scope of this research project. Therefore, other methods were explored and finally used to calculate the change in volume of Le Petit Buëch river.

The first method to calculate the difference will use a tool available in PhotoScan. Like the transects analysis described above, for volume calculation it will be drawn a polygon including all the river area and surrounding woods, excluding only the flat fields and human infrastructure. It is possible then to export and import the shapefile in other PhotoScan projects for a coherent analysis. Moreover, multiple polygons have been created to study the volume loss and material accretion not only for the whole area but also focusing just on the river banks. This will give a more understanding whether the potential loss or gain is present and correct on the river banks too or if it is just a wrong estimation of the software due to the presence of the vegetation.

The reason behind the choice of this tool resides in the easiness to use and to test the reliability of PhotoScan in slightly more complex analysis operation. In fact, the measuring tool offers basic but interesting options, giving the user the possibility to set the base plane of analysis. The options are three: (1) a “best fit plane” is created by the program according the position and height of the vertex of the polygon drawn, (2) a “mean level” plane that set the mean height of the model as the height of the plane and (3) a “custom level” plane where the user can set whatever height he wishes. The results are immediate, and the program returns three values: the volume above the plane, below it and the difference between the two. The analysis will be carried out only on the 2016-2017 datasets, as the only models accessible to the author.

On the other hand, the second method used a more reliable tool for studying river morphologies, the Cut/Fill tool available in ArcGIS with the Spatial Analyst license (How Cut/Fill works). This tool, when applied to river areas, allows to highlight the areas where there has been a gain or loss of material. It needs two rasters as inputs and the author had access to the previous DEMs processed by Hemmelder, allowing a temporal analysis of the volume change in the two river areas. It returns a new raster with three categories: Net Gain, Unchanged and Net Loss. The main downside of this method is that it doesn’t immediately return the Net Gain/Loss values, as those are needed to be calculated manually afterwards. To calculate them, the Summarise Statistics tool is used.

Differently from the first method, here the area studied will be only the river banks area, ignoring the surrounding vegetation. This because of the input used, two DSM, which are not ideal when trying to calculate the deposition and loss of material in areas with highly dense vegetation.

8 Results

In this section the results will be presented of the analysis carried out according to the guidelines given in the previous paragraphs. However, it will be shown first the positional accuracy of the DPGS and subsequently a qualitative description of the catchments will be conducted.

The outputs of the workflow shown previously that will be used for the analysis and discussion are the OrthoMosaics and DEMs exported from PhotoScan. The two datasets have different coordinate systems, with the DPGS location of the 2016 dataset using "WGS 1984", while the 2017 has "RGF 1993 Lambert 93". Furthermore, the OrthoMosaics and DEMs from Hemmelder et al. (2018) are in different reference system too, "WGS 84/ UTM zone 31 N". Therefore, both mosaics and DEMs from 2017 have been projected in ArcGIS with the same reference as Hemmelder's end products.

8.1 DPGS precision and products resolution

The outputs yielded by PhotoScan are all extremely high-quality products. Some of them, specifically the two 2016 dataset, show a higher error of the DGPS location but still with a great final resolution. On the other hand, both 2017 dataset show a very small error in the location of the DGPS and a great resolution as well.

PhotoScan provides some options to check the accuracy of the DGPS in its reference pane. Moreover, another tool allows the user to visualise directly on the orthophoto the amount and magnitude of the error (**Figure 16 and 17**). The error given for the DGPS (in m and pix) is shown below as follows:

- La Bâtie-Montsaléon:
  - 2016: 0.61 m and 1.9 pix
  - 2017: 0.03 m and 0.63 pix
- Chabestan:
  - 2016: 0.28 m and 0.764 pix
  - 2017: 0.09 m and 1.416 pix

Behind this huge difference between the 2016 and 2017 dataset there are several explanations. The main reason for La Bâtie-Montsaléon 2016 can be searched in the low number of photos available (295) and the quality of some them. The number of projections for each marker is quite low and what is striking is that the photos with the highest error are also the one with the at least 10 projections. This, combined with high error easily

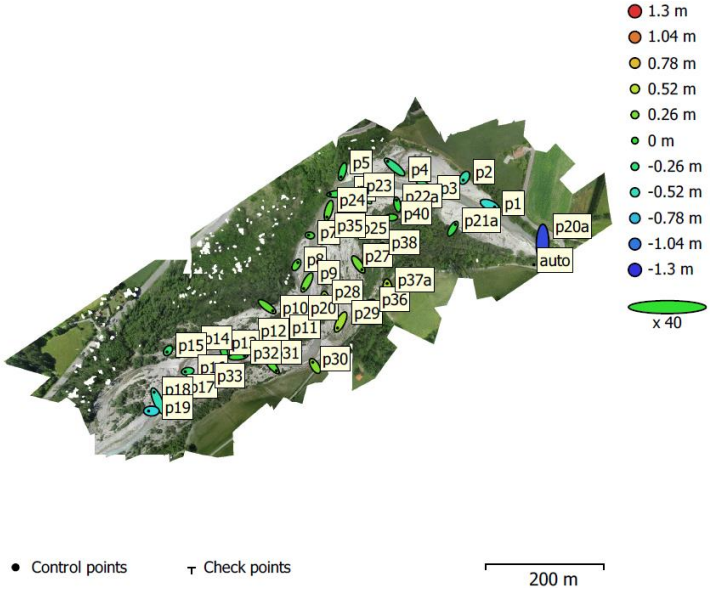

Figure 17 GCP locations and error estimates at La Bâtie-Montsaléon. Z error is represented by ellipse color. X,Y errors are represented by ellipse shape. Estimated GCP locations are marked with a dot or crossing

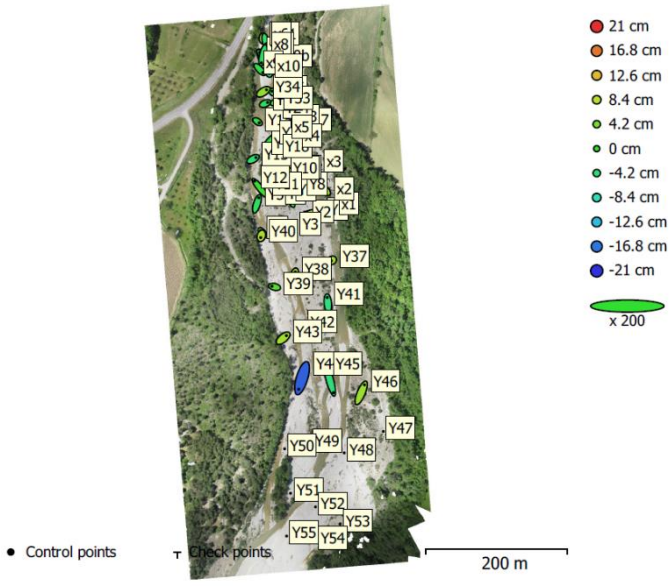

Figure 16 GCP locations and error estimates at Chabestan

obtainable from markers with less than 10 projections and low-quality imagery (blurred, hidden by the vegetation), is possibly the main reason behind the high average location error of the markers.

Differently, the Chabestan 2016 dataset has more than double the photos but still a high location error. This might have to do with the fact that the imagery was captured in two different days, with different markers in different location. In one of the first run, if tried to process the dataset all at once, the error given was above the meter. Luckily, PhotoScan allows the user to process the data in different batches and then merge the resulting products. The result, as shown above, is much better but still inaccurate compared to the 2017 dataset. Lastly, is good to point out that this results are the best the author could get out of the 2016 dataset, even with manual position of each marker in each photos, differently from the 2017 dataset where the program figure it out by itself the almost perfect location of the markers, limiting any external interference to correct only clearly offset position of few markers.

Regarding the resolution, the products yielded are in line with the initial expectations, as seen below:

- La Bâtie-Montsaléon:
  - 2016: DEM (46320x38695, 2.32 cm/pix), OrthoMosaic (44338x28652, 2.32 cm/pix)
  - 2017: DEM (30388x128241, 2.76 cm/pix), OrthoMosaic (30388x25936, 2.76 cm/pix)
- Chabestan:
  - 2016: DEM (17070x51552, 2.79 cm/pix), OrthoMosaic (16771x51551, 2.79 cm/pix)
  - 2017: DEM (12192x24152, 3.36 cm/pix), OrthoMosaic (121027x24152, 3.36 cm/pix)

Yet, all the DEMs and OrthoMosaic present holes that couldn't be filled. These holes are a marginal problem overall, as they are not hindering the interesting areas for the analysis but are located mainly on the edges and in areas of dense forest, where the program struggles to find common point between images.

8.2 Qualitative river description

8.2.1 Chabestan

The datasets cover an area between, approximately, 0.28 and 0.3 Km^2. The 2016 dataset is bigger and is comprised of further another downstream part of the river, consequentially it has been clipped to the same extent to speed up the data processing and have a homogeneous analysis between the two datasets. The river OrthoMosaics is described in its flowing direction, upstream (north) to downstream (south). Of interest are the two overlap maps obtainable from PhotoScan (**Figure 18**), showing the difference in overlap between the two datasets. Noticeable is the higher overlap in the 2017 dataset, even though the number of photos is inferior than its 2016 counterpart (711 vs 379). The higher overlap in this case might be due to smaller area taken into consideration. As a matter of fact, the 2016 OrthoMosaic present a high number of holes, especially in the peripheral areas of the mosaic. Moreover, the Chabestan 2016 dataset is the only one that has been captured in two different days, possibly leading to a higher inaccuracy (e.g. different light, atmospheric condition and also GCPs) of the program when trying to overlap the imagery and build the OrthoMosaic. Thus, the 2016 has been clipped to a similar extent as the 2017 OrthoMosaic, simplifying the visual analysis and reducing the processing time of the data for the quantitative analysis.

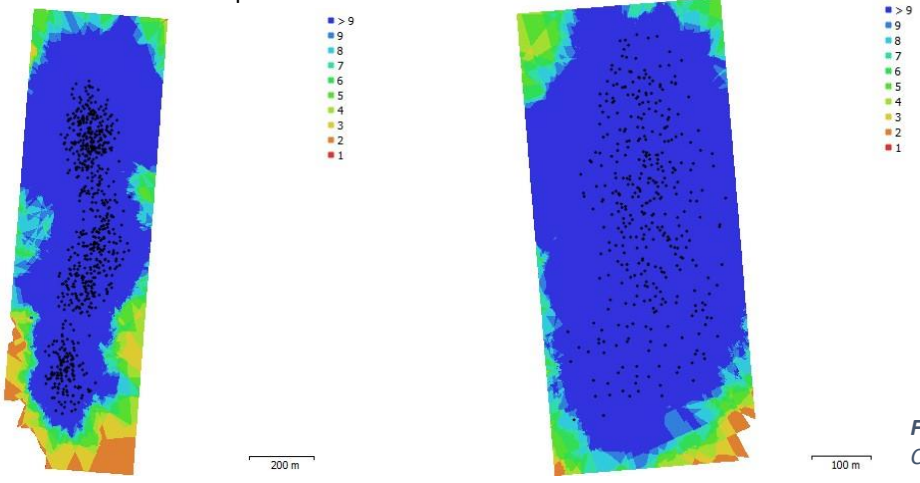

***Figure 18** Overlap difference between Chabestan 2016 and 2017 imagery*

8.2.1.1 Chabestan 2016 – 2017

The visual comparison of the two datasets doesn't show huge differences in the two river paths. The main stem divides in two (2016, 2017 – B1) and the two branches continue till they re-join some hundred meters southern (2016, 2017 – C3). These two branches saw the most changes over the year, with a lot of sediments deposited on the western banks of the river (2017 – B2, B3) and a further division in two of the western branch (2017 – C3, B3, B4). On the eastern branch the major observable change is the creation of two islands that "braid" the river path. Here the erosion is clear, but the loss of volume is limited. On the contrary, the river bed seems to have gained some volume with the creation of these two new small islands.

Lastly, the opening of multiple branches seems to be the main cause for the width shrinking of the river path and perhaps the raising of the river bed too, as the colour of the water got darker over the year, suggesting a lower height between the river bed and the surface.

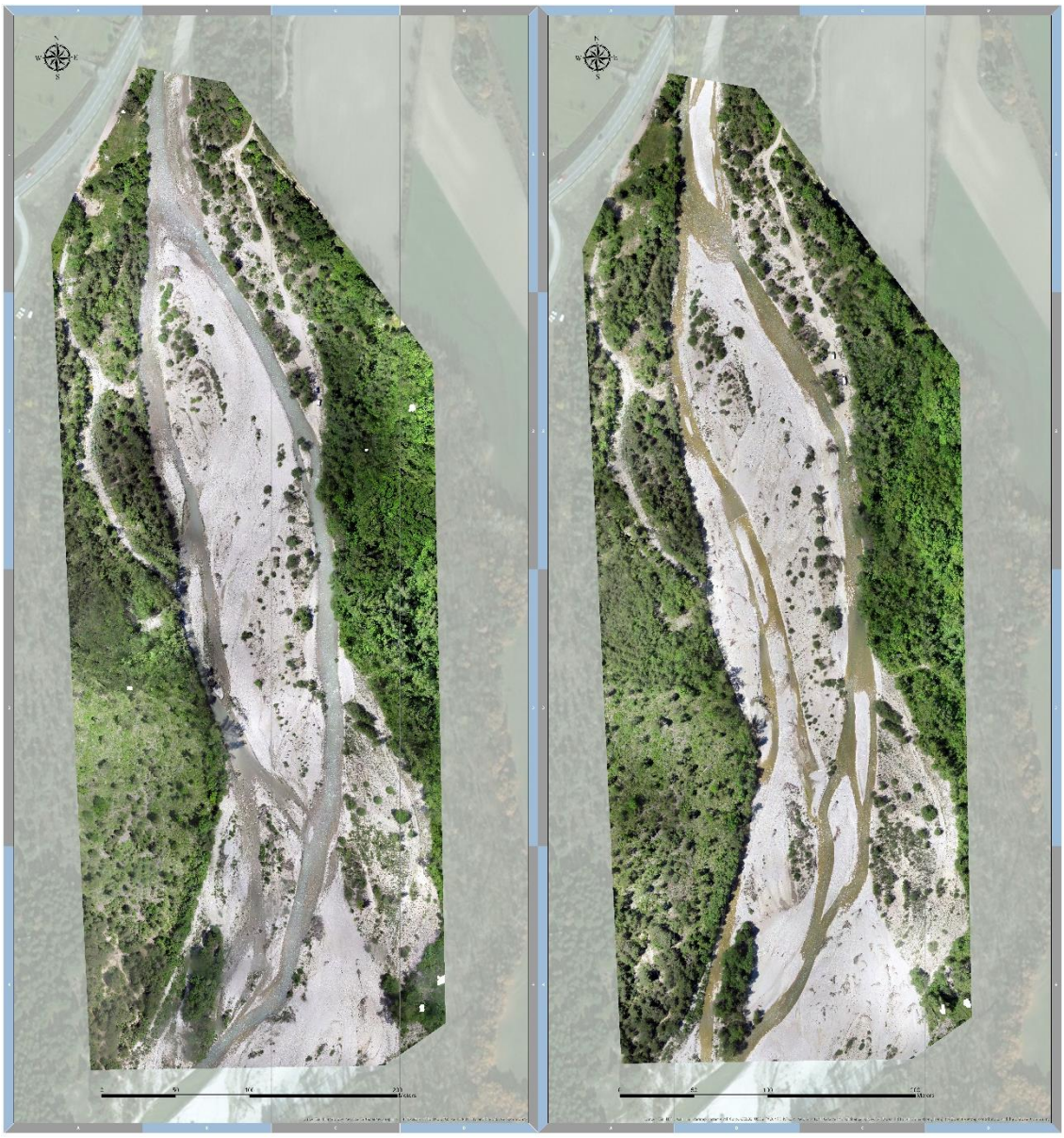

Figure 19 *The two OrthoMosaic of the Chabestan study area, 2016 and 2017*

8.2.2 La Bâtie-Montsaléon

The datasets cover approximately the same extent area, about 0.3 Km^2. The river OrthoMosaics is described in its flowing direction, upstream (east) to downstream (west). Of interest are the two overlap maps obtainable from PhotoScan, showing the difference in overlap between the two datasets. 2017 dataset shows higher and

homogeneous overlap between the images, resulting in a more defined extent of the OrthoMosaic and less holes in it. On the contrary, 2016 dataset show less overlap in the areas next to the river, resulting in a less defined extent and numerous small holes in the surrounding areas. In this case the large difference in the number of photos available and processed for each dataset might be the reason difference in overlap: the 2016 dataset is composed of only 295 photos while the 2017 has three times more photos available, 842.

Lastly, it is important to note that, as the Chabestan datasets, these two sets of imagery were taken during the dry season of the river (summer), therefore the discharge is quite low. This means that the river banks are drier and therefore the morphological characteristics are highlighted even more than usual.

8.2.2.1 La Bâtie-Montsaléon 2016 – 2017

The comparison between the datasets shows clear changes in the river path from one year to the other. Starting upstream (D2) it is noticeable that, while the main stem maintained mostly the same path, two new branches opened on the northern side (2017 - C2 and C1) and southern side (2017 – C2) of the river, following the very edge of the vegetation on the border between the river banks and the anthropic areas surrounding it. Of major importance (and something that needs to be addressed in future) is the erosion process of the northern branch, that distinctly closed the gap with the nearby railway line. The re-opening (it seems like that the branch was already there, 2016 – C1) let the water divide from the main stem and reduced its discharge. Without calculating the height of the river bed, it is safe to say that there has been a height reduction, as the colour of the water is more brownish, suggesting lower distance between the river bed and the surface. Similarly, the southern branch eroded part of the vegetation (2016 – C2) and re-join the other branch straight away some meters further away (2017 – B2). In this quadrant (2017 – B2) it is possible to appreciate another clearly visible change in the path of the river, with what seems more vegetation eroded on the western side of the river. The river paths continue broadly with no major displacement, with a minor reduction in width and a slight reposition of the last meander captured by the imagery (2016 – C3, 2017 – B3) now a little farther away from the nearby agricultural field.

Figure 20 *The two OrthoMosaic of La Bâtie-Montsaléon study area, 2016 and 2017*

8.3 River path displacement

8.3.1 Chabestan

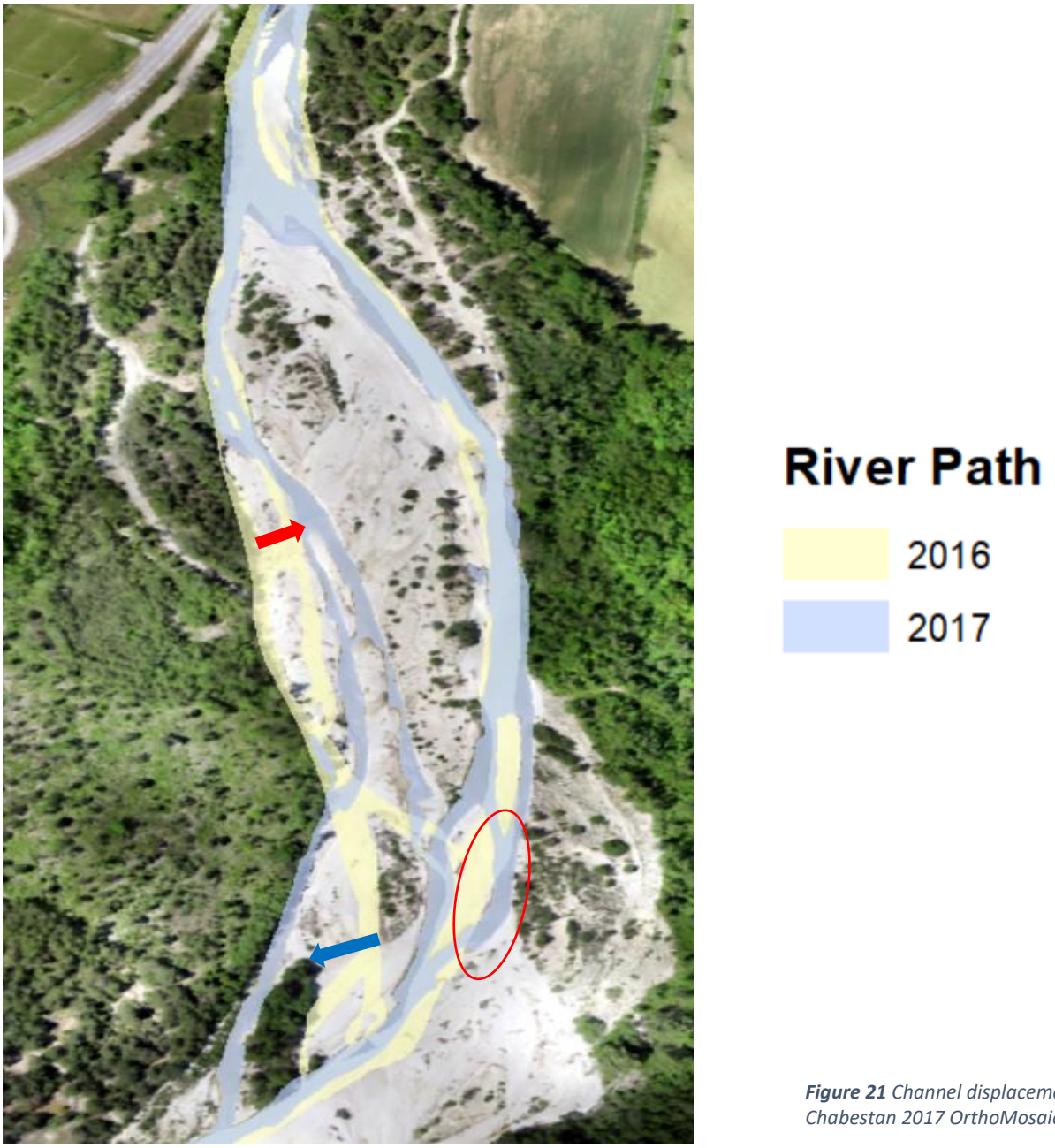

Figure 21 *Channel displacement on Chabestan 2017 OrthoMosaic*

The visual comparison of the OrthoMosaic helped in spotting major differences between the years, preparing the terrain for the channel displacement analysis. In fact, the visual comparison made possible to differentiate some inactive channels from others. As seen here, the two digitized river paths are overlaid on the 2017 OrthoMosaic. The differences in the path are not great but in one year it is noticeable how the sedimentation processes established and increased the size of the banks on the western branch and the movement of its path ~30m towards the other branch (Red arrow).

Sedimentation was intense also on the eastern branch and in the southern part of the study area. If the eastern stem didn't see huge changes in its path over the year, it is also true that new islands formed in its path (red circle). This sedimentation process is even more noticeable where the two main branches meet. A new island formed and, as a result of that, the western branch further divides digging a new path along the forest line (blue arrow). Again, the river path moved about 30 m, this time in the opposite direction.

8.3.2 La Bâtie-Montsaléon

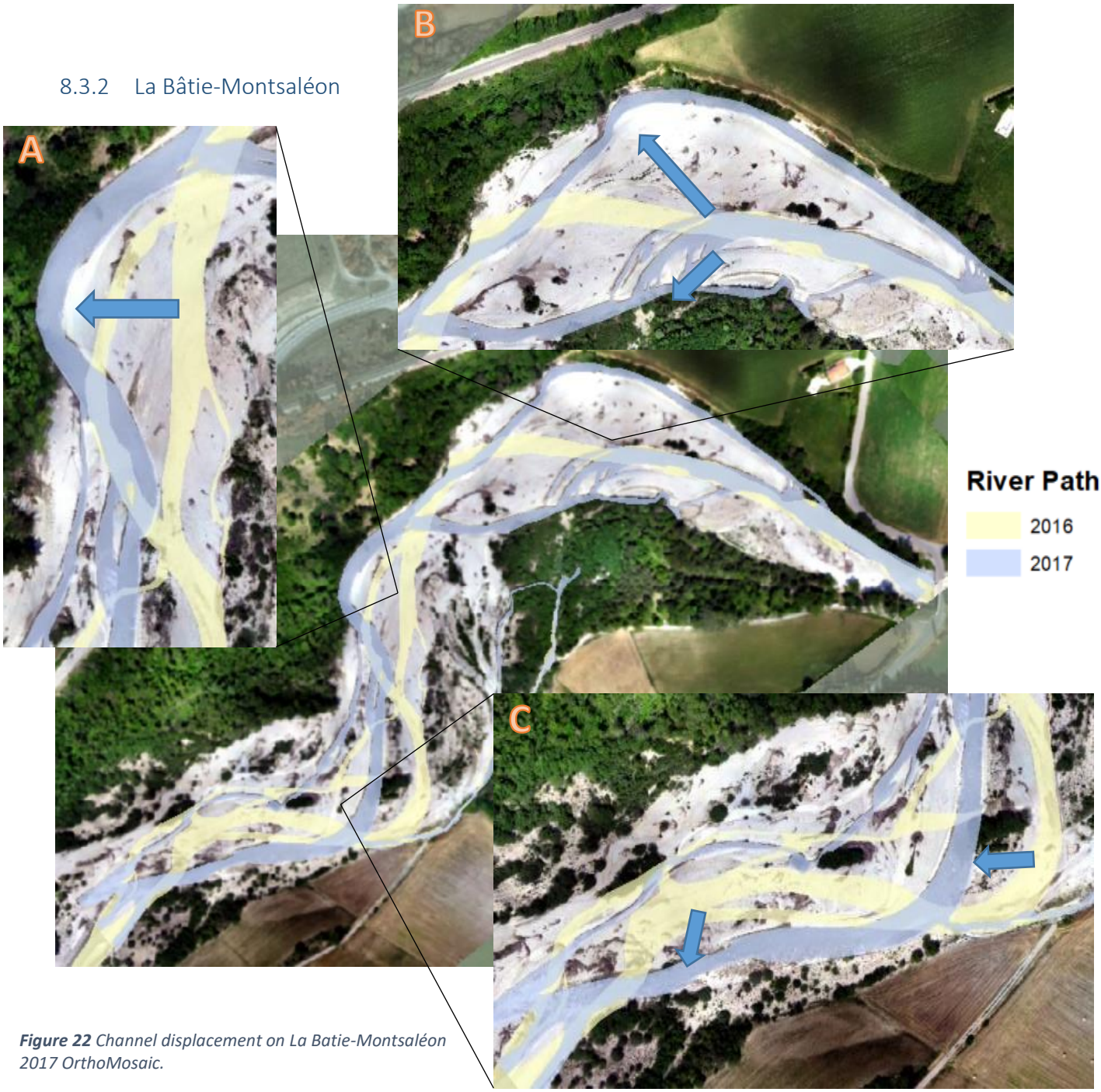

Figure 22 *Channel displacement on La Batie-Montsaléon 2017 OrthoMosaic.*

The path displacement analysis confirms the results of the visual comparison of the two OrthoMosaic. This catchment underwent great changes over the year with the opening of new branches and heavily eroding the banks in the middle and upper section of the catchment (A and B). These locations saw a continuous erosion and in the last years (Hemmelder et al., 2018) and the threat related to nearby infrastructure (B, insert approximate displacement) is certainly a critical concern that must has to be addressed. Moreover, the loss of vegetation (A, insert approximate displacement) further increase the instability of an already fragile environment and the danger of destructive flooding event in the area.

However, location C shows some improvement as the main trunk of the river moved away from the nearby fields while heavily eroding the southern banks of the catchment (insert approximate displacement). This renewed erosion process let the river path acquire a more meandering shape compared to the other location at Le Pont du Chabestan. Yet, new branches are opening and started to flood the woodland in between location B and C. This is another issue that must be addressed as, considering the fragility already shown in other areas of the two catchments, not even vegetation is able to stop the river to constantly transform and open (or re-open) new branches more and more close to the surrounding anthropic areas.

8.4 Profile analysis

In both catchments is possible to observe the effect of bank erosion and sedimentation. Both areas underwent a great transformation over the year, especially the river study area at La Bâtie-Montsaléon. It was already clear with the visual comparison of the OrthoMosaics that both withstood to strong erosion processes, however it possible to fully grasp the effects only by studying the DEMs and derived slope maps.

Moreover, because the OrthoMosaics are extracted from the DEMs, this allows for the analysis to be carried out is directly in PhotoScan as here the height information is kept in the OrthoMosaics cells too.

8.4.1 Chabestan

Figure 23 *Transects drawn in PhotoScan at Chabestan 2016 and 2017*

In the Chabestan catchment seven transects were traced in different location to compare the erosion effect (if any). The transect 1 to 4 are in similar location as in the analysis carried out by Hemmelder et al. (2018), for further analysis on larger time scale. However, the area underwent changes also in other locations, therefore the addition of three new transects (5 to 7).

As pointed out in the initial paragraph, the transect analysis is not influenced by the different reference planes. PhotoScan quite cleverly understand that the transects drawn on the OrthoMosaic should be studied by their height on the surface and not by the height they were drawn (which would be 51 m above the surface and therefore returning a blank profile graph).

The graphs presented below also show the “noise” produced by the water and the interference of vegetation. This is not a major problem, as the banks are still recognisable, but gives a hint on where the difficulty lies when analysing braided river systems and river systems in general.

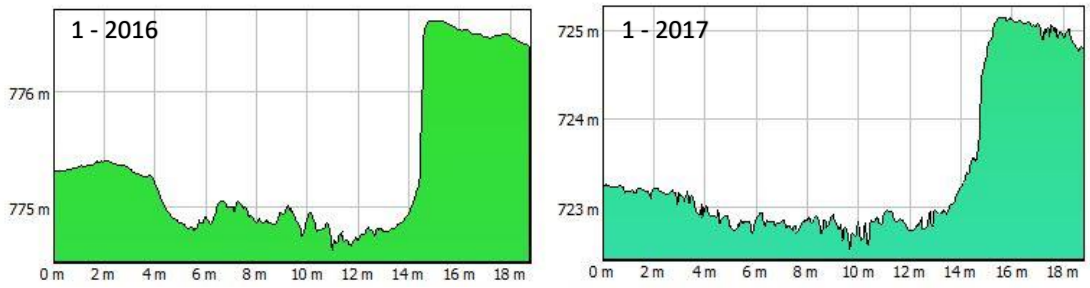

Figure 24 *Chabestan transect 1*

The first transect shows how the eastern branch of the Buëch river in Chabestan underwent light erosion processes. The right bank kept its height and slightly gained some terrain. On the other hand, the left bank has seen more aggressive erosion, with its height reduced, but not a clear movement in that regard.

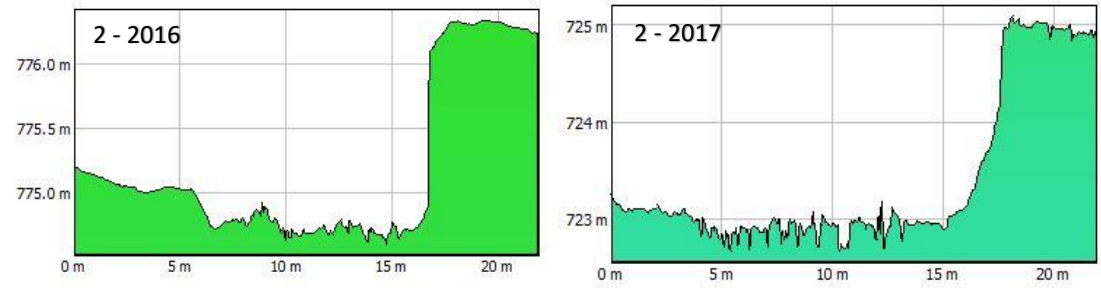

Figure 25 *Chabestan transect 2*

The second transect shows a behaviour very similar to the first one. Almost no change on the right bank and loss of height in the left, but not a clear displacement.

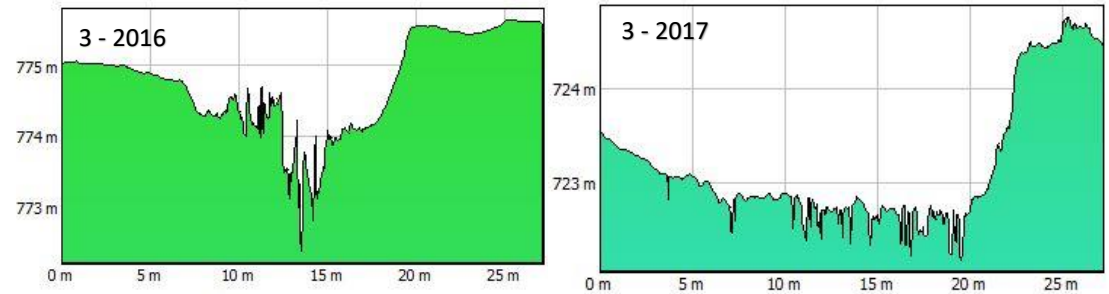

Figure 26 *Chabestan transect 3*

The third transect, meanwhile, underwent major changes over the year. The channel widened and a lot of terrain has been lost. On both banks there’s a loss of about 4m, with the left bank mostly affected by the change.

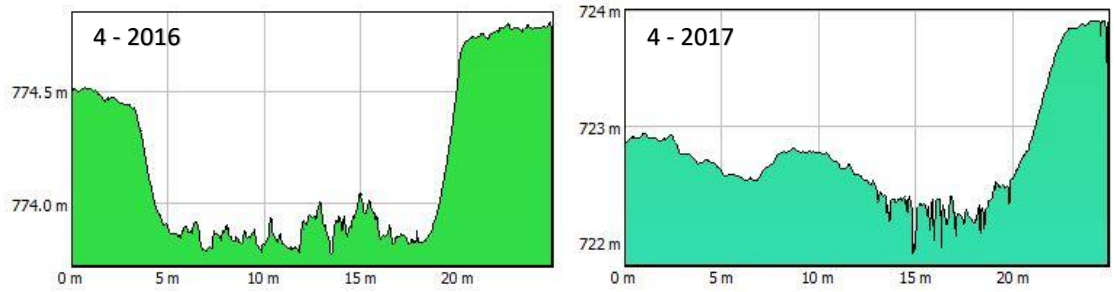

Figure 27 *Chabestan transect 4*

The fourth transect reveals the first, major changes on the eastern branch. In 2016 the profile's shape was the same the first three transects, but the displacement of the channel over the year is clearer. While the right bank has been left almost untouched, the left bank has seen a growth and gained terrain, about 7m narrowing the channel. Yet, it is still possible to appreciate the small branch that was part of the 2016 path in the 2017 graph, around the 5m height on the transect. This is merely impossible to notice with the OrthoMosaic and this type of analysis, helps once again, to study the river behaviour not only from year to year but also in predicting future, possible, openings of new (or old) branches.

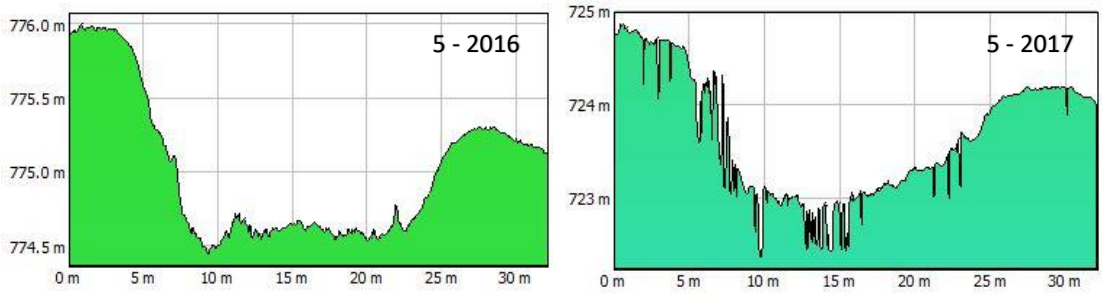

Figure 28 *Chabestan transect 5*

Moving to the western branch, here the analysis of the bank displacement is sparser and hard to perform. The overhanging vegetation on the left side of the channel is to thick and wide to have an accurate estimation of the displacement, but two location where free of vegetation and suitable for it. The fifth transect display a narrowing of the channel, already clear from the OrthoMosaic. The left bank didn't undergo much changes, more vegetation grew on the waterfront and a small islet has formed. The right bank gained a lot of terrain and reduced the width of the channel. From 2016 to 2017 the channel went from about 10 m width to about 3 m.

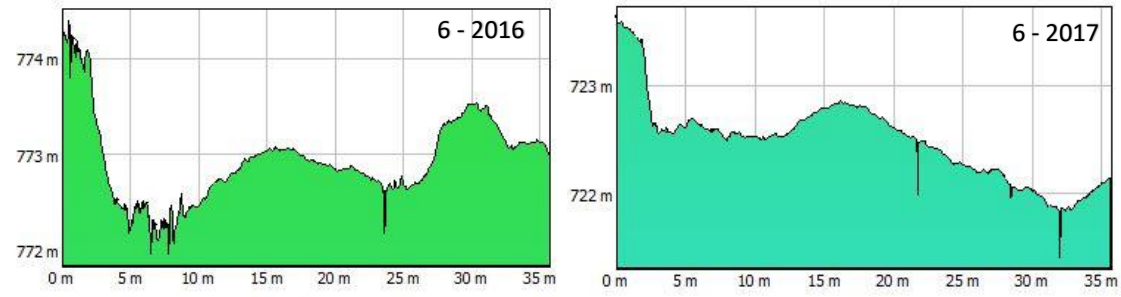

Figure 29 *Chabestan transect 6*

The sixth transect is very much of interest, as here the bank displacement is clear from the OrthoMosaic and the morphology completely changed from 2016 to 2017. The channel in 2016 was divided in two by an isle and only a small portion of the eastern branch was left in 2017, while the western stem has been replaced by a new great bank and the channel moved further to the east of about 15 m. Likewise for transect 4, also here the 2017 graph shows that the old channel is still there. Meanwhile, the right bank underwent great morphological changes, and

the formation of a new isle with low heights suggest that it is deemed to disappear over the year in the next high-discharging events.

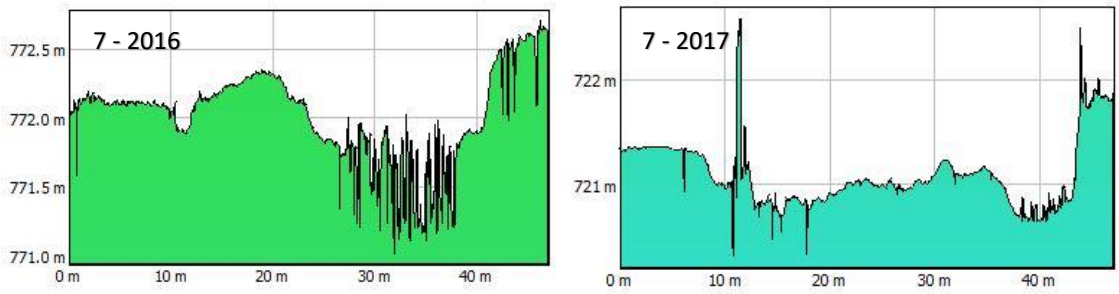

Figure 30 *Chabestan transect 7*

Lastly of note, the seventh transect is in an interesting location, at the confluence of the two main branches. First of all, it is to note that in the 2017 graph, the spike around 10 m is a tree. The river here underwent great changes and it is possible to observe both sedimentation and erosion processes at work. The massive isle that was separating the two branches has been eroded from the western branch, as seen for transect 6, but without causing major height loss of the bank. However, the erosion of the eastern branch on it has been stronger and resulted in a loss of about 5 m of terrain. However, what has been lost there has been regained in the form of a new isle, that cuts the eastern branch.

8.4.2 Slope map analysis

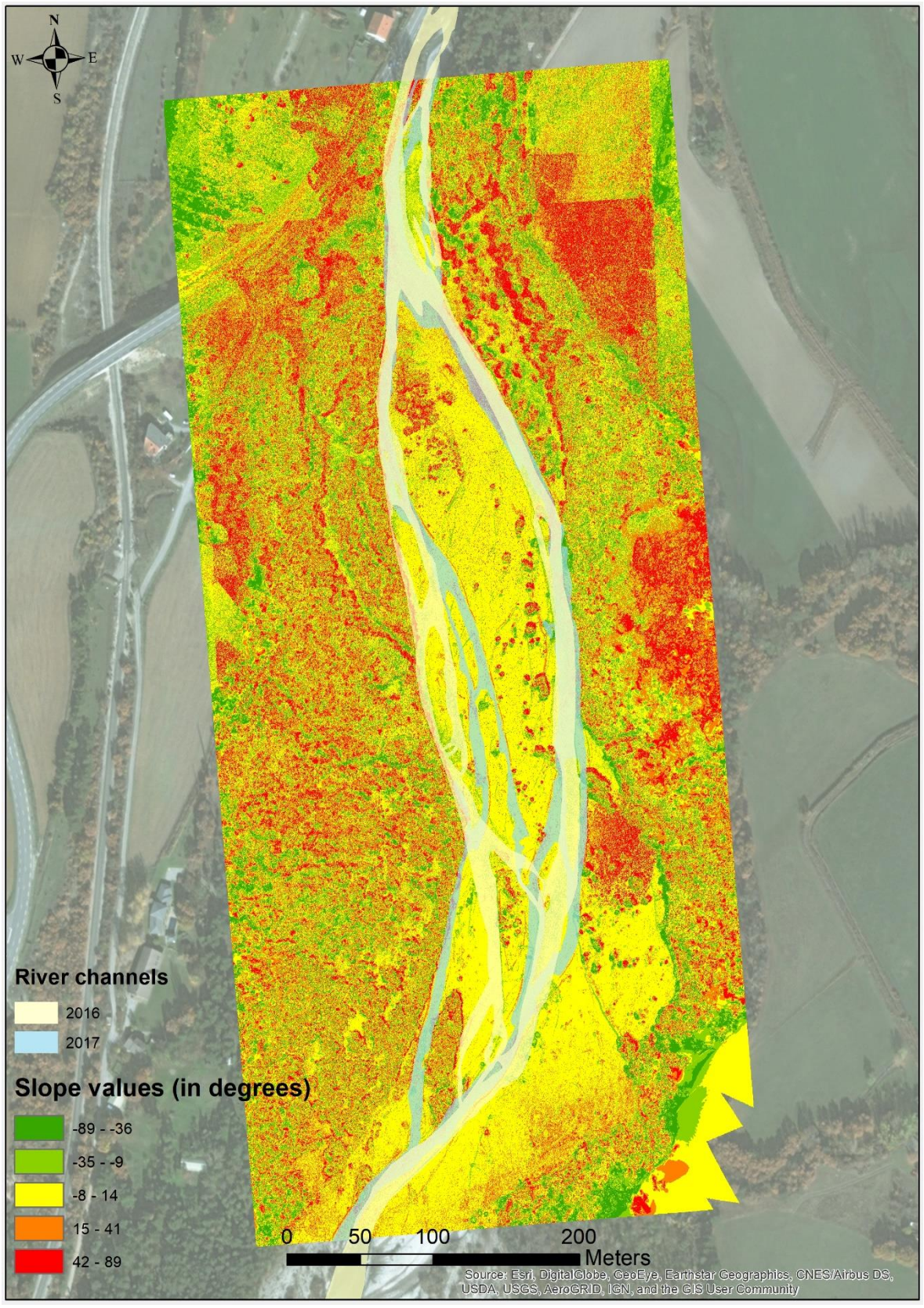

Figure 31 *Difference in slope map of Chabestan study area*

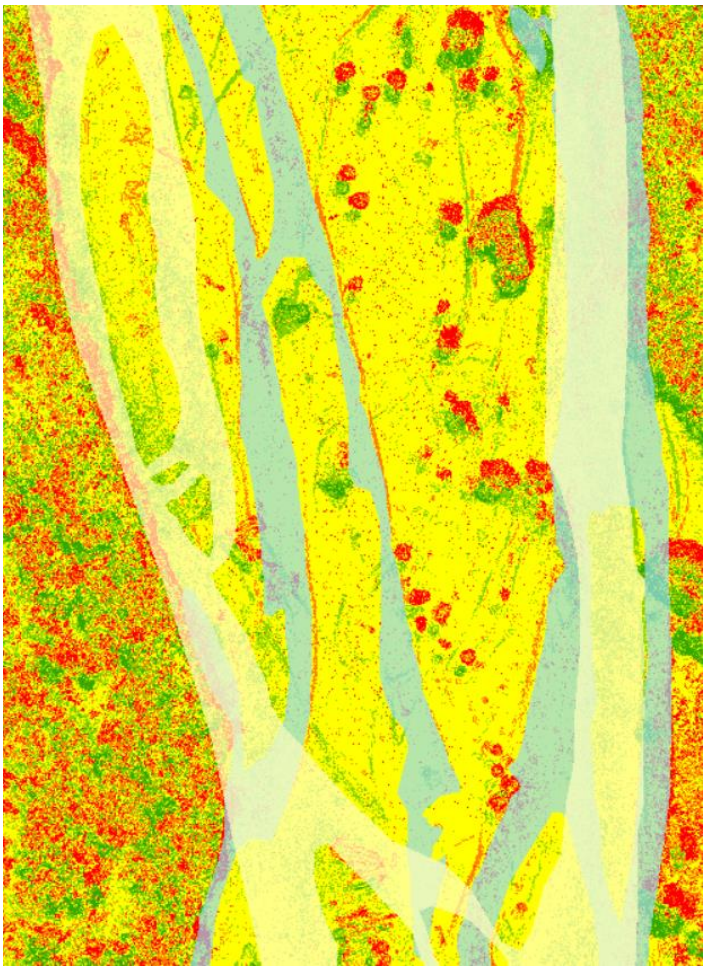

Figure 32 *Highlighted location of the slope map.*

It is possible to observe the old channel partially filled with sediments next to the tree line, the new banks that formed and some old inactive channels on the right-hand side of the current channel

The use of slope maps can help in the bank erosion analysis. Calculating the difference in slope between the 2017 and 2016 dataset it is possible to obtain a slope map where it is possible to appreciate the changes in slope degree and therefore where bank erosion occurred. Moreover, it is possible to find morphological features that might have slipped away in the visual comparison of the OrthoMosaics, such as inactive branches and newly created banks. The colour of the map must be interpreted as follows: greenish areas are where erosion took place and the redder it gets, the less erosion occurred.

This method is more reliable as it calculates the relative difference instead of calculating the absolute difference as it would be when calculating the heights of two DEMs. Besides, calculating the difference in height is not suitable in this study case, as the DEMs are DSM and not DTM, with the vegetation covering some areas and the height values of the water creating some noise in the final output.

In Chabestan the slope map confirm that the erosion of the banks has been feeble and that the vegetation and terrain resisted it over the year. As a matter of fact, the catchment seems to have slightly “gained terrain” and saw accretion of the banks.

8.4.3 La Bâtie-Montsaléon

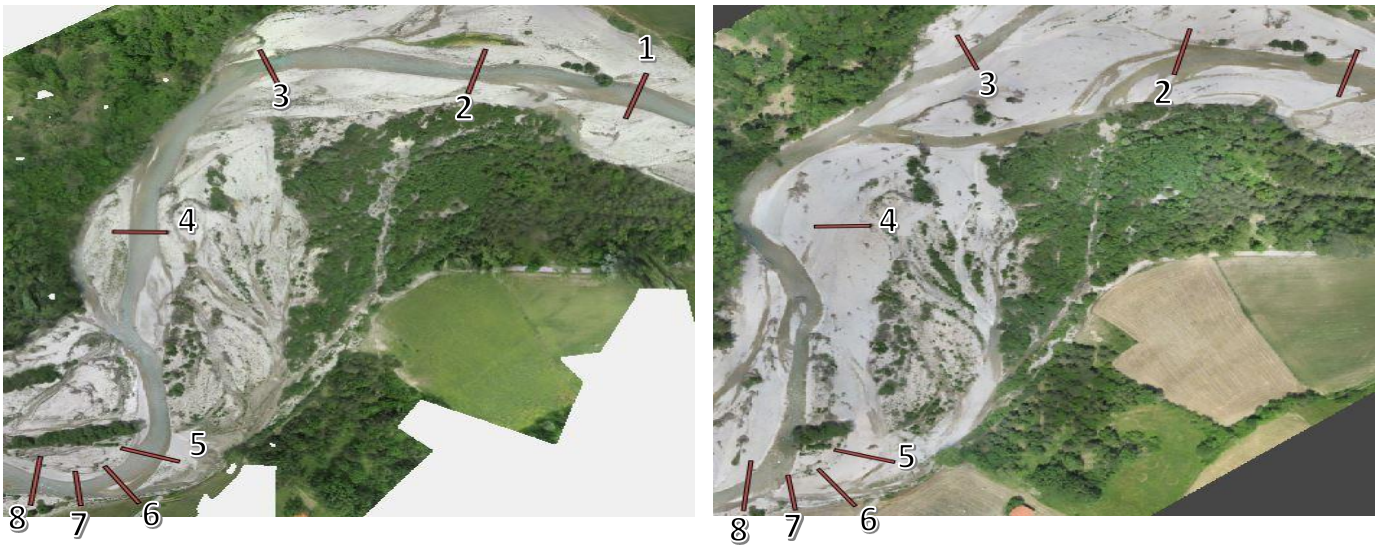

Figure 33 *Transects drawn in PhotoScan at La Bâtie-Montsaléon 2016 and 2017. It is already possible to see the great morphological changes the river underwent over the year*

The study of La Bâtie-Montsaléon is possibly more interesting to analyse, as the river here underwent intense transformations in its path. Moreover, the path of the river as fewer branches and it's easier to compare the displacement.

In addition, it is important to note that this profile graphs have a much more accentuated difference than it is. The Y axis hardly have differences of 2 meters in their min-max values and most of them are in range of centimetres to a meter, quite dissimilar from the Chabestan study area.

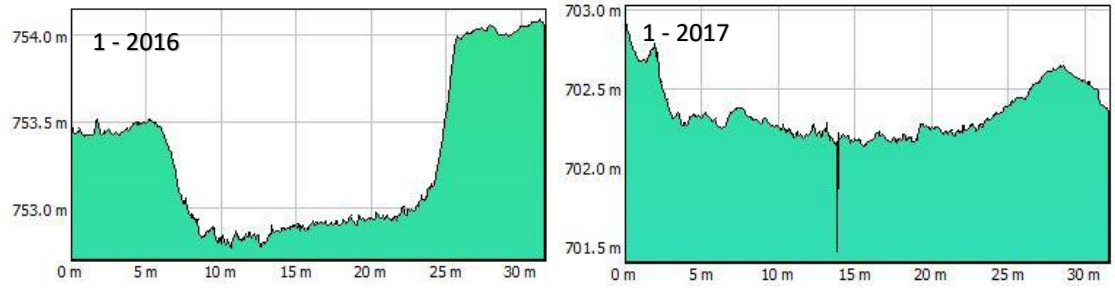

Figure 34 *La Bâtie-Montsaléon transect 1*

The first transect displays a slight widening of the channel, about 2 meters per side. Despite the look of the profile graphs, this is the transect that underwent the least changes of the year.

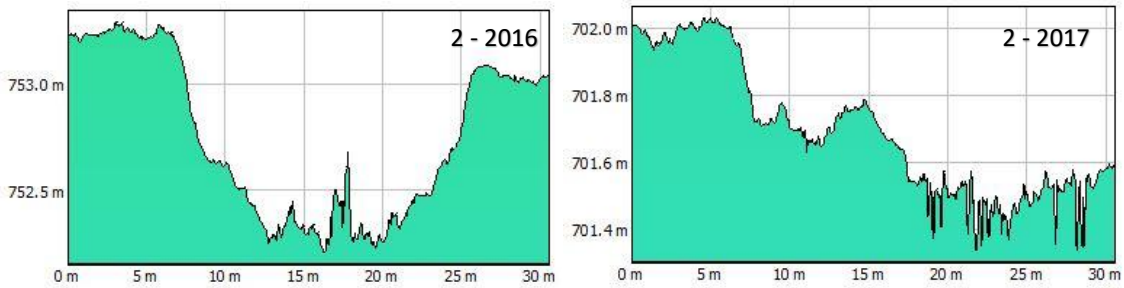

Figure 35 *La Bâtie-Montsaléon 2*

The second transect is more interesting, as one of the end points in the 2017 OrthoMosaic lies in the river. Here the river path changed direction more than displaced its banks. If the left bank has remained almost the same, with a slight raising of the banks, the right bank moved slightly farther away and widened the river channel. Yet, it is hard to express the magnitude of the erosion, as the river did not create new paths but re-opened inactive channels.

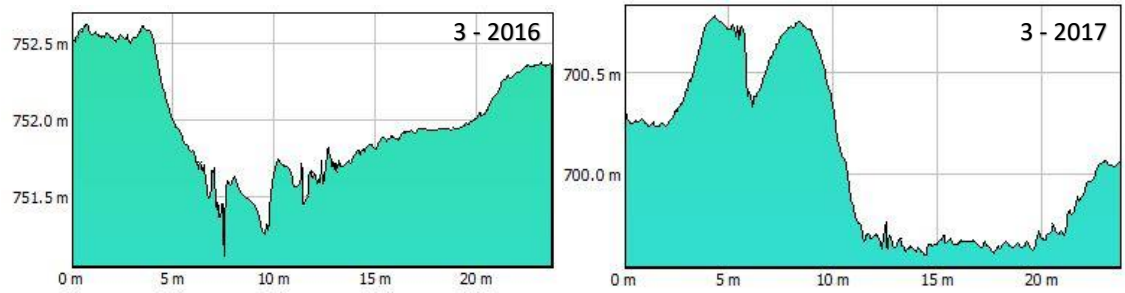

Figure 36 *La Bâtie-Montsaléon 3*

The third transect is in an interesting location. The 2016 measurement was made on the single stem of the Buëch river that was cutting the whole area, while the 2017 measurement is taken on one of the two branches that separate at the start of the studying area. Therefore, it's hard to define if there's channel displacement and how strong it is. Despite the look of the graphs, the differences are minimal, with a gain of terrain on the left bank and a narrowing of the channel of about 3 meters.

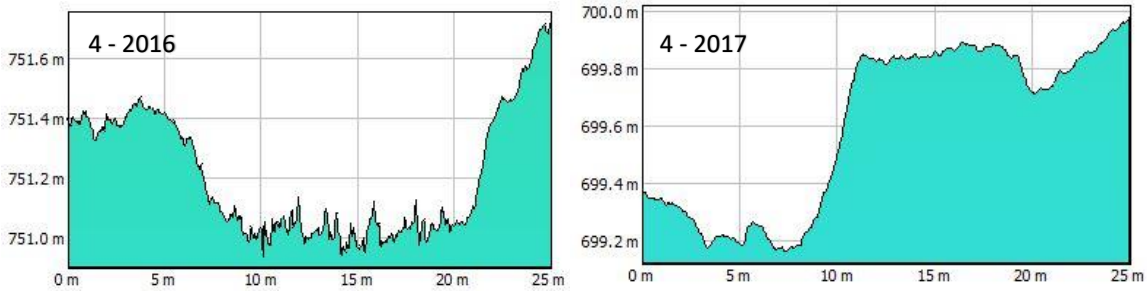

Figure 37 *La Bâtie-Montsaléon 4*

Similarly to the sixth transect in the Chabestan study area, also this location underwent great changes over the year, with the complete displacement of the channel and the accretion of the bank volume. If the 2016 profile display a "natural" river channel with the high banks on the sides, the 2017 profile is very peculiar. In fact, over the year the river bed has been filled only partially, leaving a lower area that suggests future re-opening in case of high-discharge events. The displacement here is huge, the greatest in both the study areas, with channel about 25 m western from its original position.

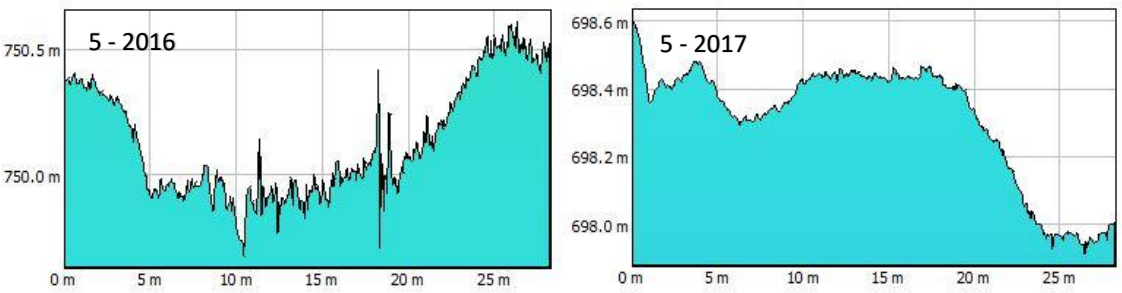

Figure 38 *La Bâtie-Montsaléon 5*

The fifth transect had a similar fate as the previous. The channel in 2017 completely displaced from its original 2016 position and it is about 15 m eastern. Like transect 4, the old channel has been almost filled, leaving only a small portion at a lower level.

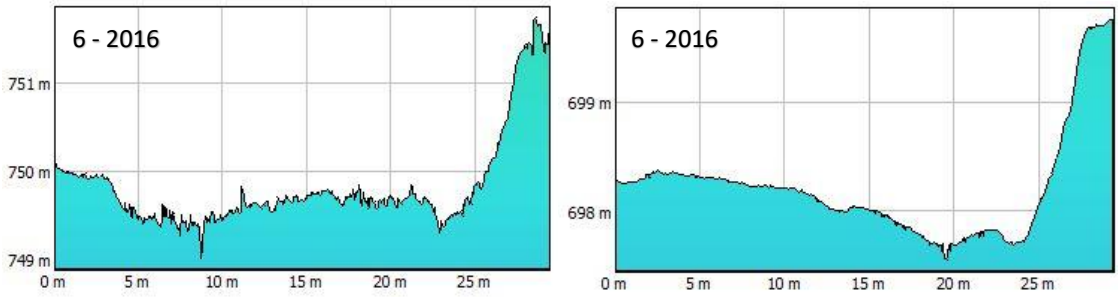

Figure 39 *La Bâtie-Montsaléon 6*

The sixth transect display, once again, how the channel moved to the east (this time about 3 meters), leaving the measured area "dry". It is interesting to note how profile kept the same shape and heights, despite the lack of a river, and also clearly shows the new small branch of the river that now run along the fields and comes from the woods. Already from the OrthoMosaic visual analysis was already possible to spot this new branch, but the profile analysis gives more insight and will allow in future to better monitor it.

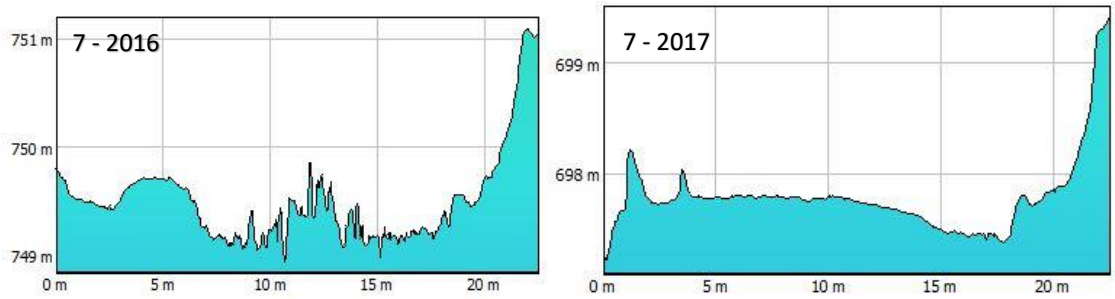

Figure 40 *La Bâtie-Montsaléon 7*

The seventh transect underwent the same changes as the previous three, especially transect 6. In the 2017 profile it is noticeable where the channel ends, exactly at the 0, while the rest of it shows the old river bed. Likewise transect six, it is possible to spot the new branch running along the fields, around 15 m on the transect X axis.

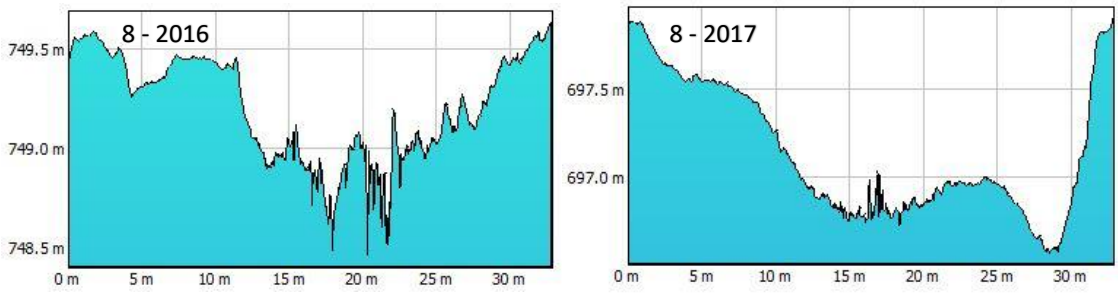

Figure 41 *La Bâtie-Montsaléon 8*

Lastly, the eighth transect saw a change of the direction of the path more than a displacement, similarly to what happened with the second transects.

8.4.4 Slope map Analysis

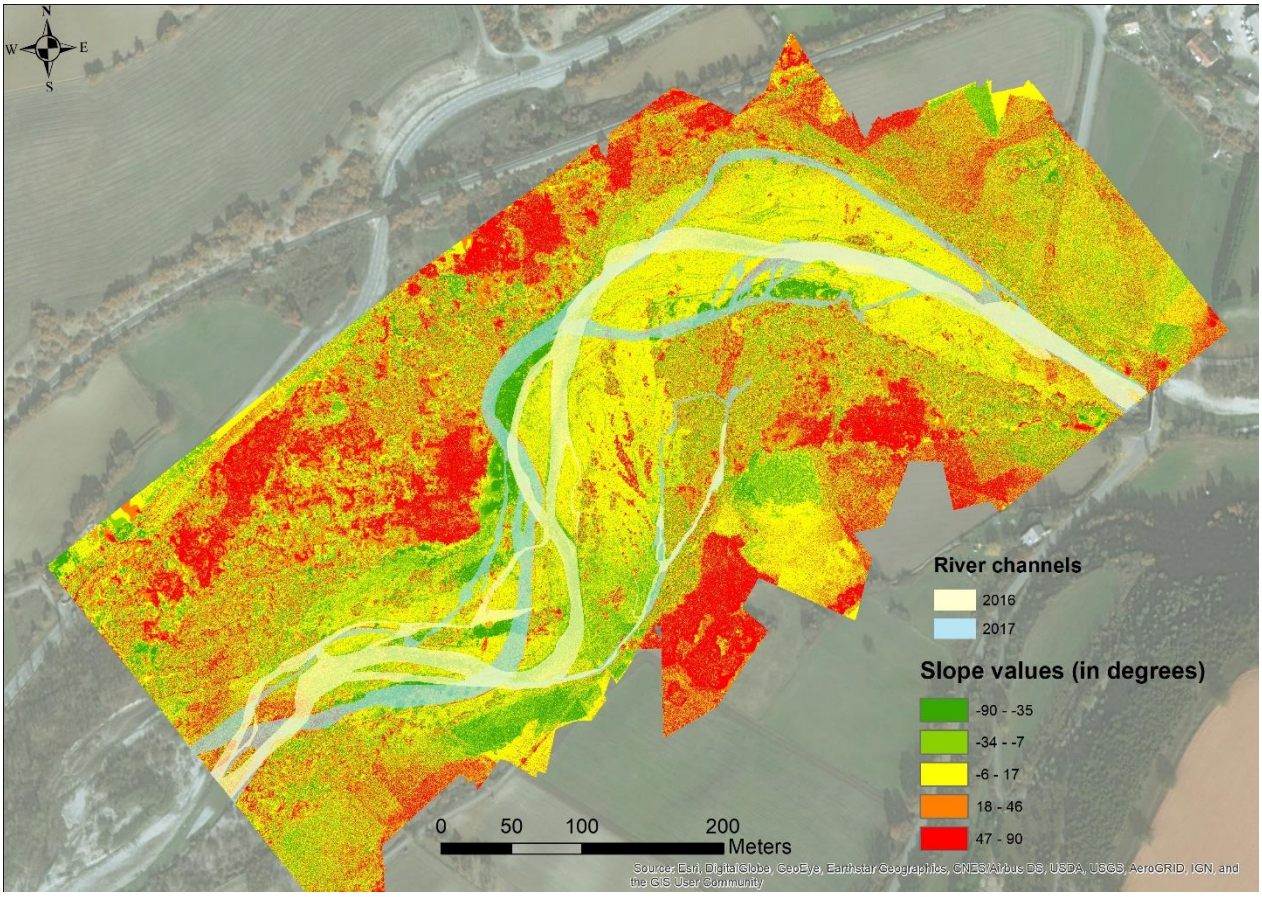

Figure 42 *Difference slope map at La Bâtie-Montsaléon*

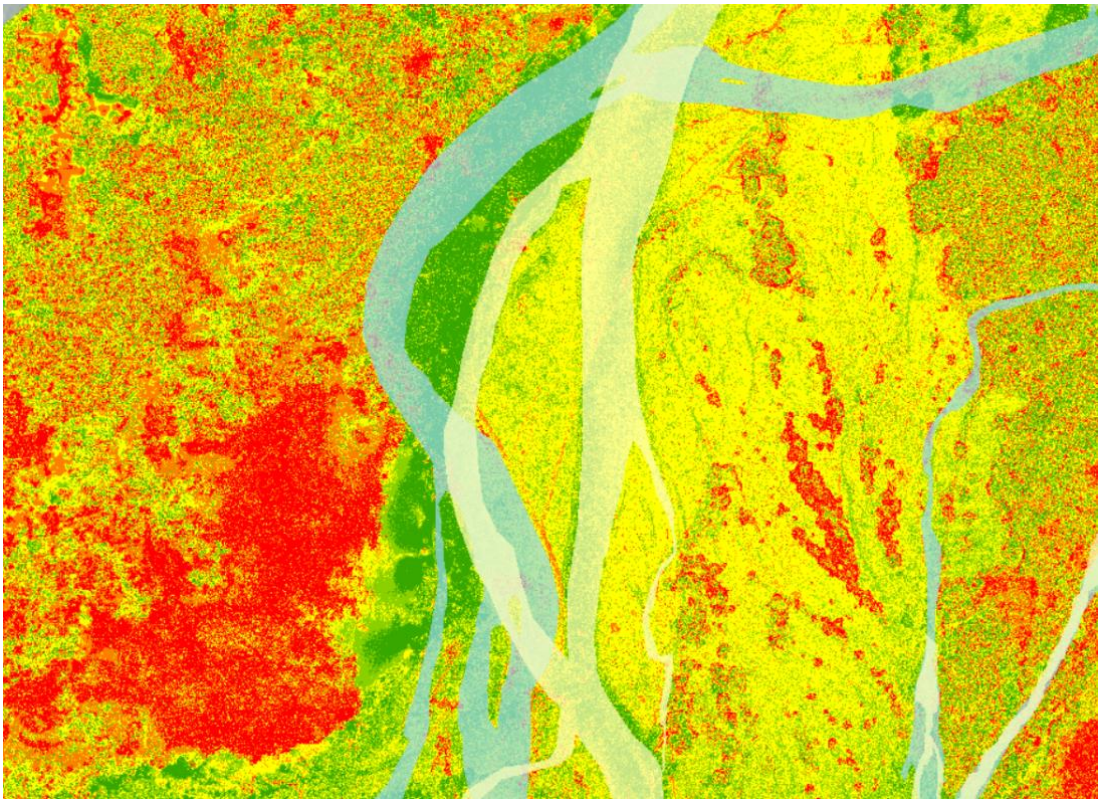

Figure 43 *Highlighted location of La Bâtie-Montsaléon slope map. It is clear the erosion occurred and the vegetation loss, while it is possible to see yet the 2016 channel (only partially filled by new sediments) and the newly created banks*

The slope map obtained for La Bâtie-Montsaléon show quite a different result compared to Chabestan. Here the erosion processes were much stronger and affected various locations of the catchment. This was already visible in the OrthoMosaics comparison, but this slope map clearly shows the intensity and extension of the eroded areas.

Like the Chabestan slope map it is possible to appreciate some morphological features, but in this one the changes were so deep that inactive channel channels were already visible from the OrthoMosaic. Moreover, here it is possible to partially see the 2016 river path. This is because the river eroded and displaced its channel leaving dry the old river bed and we little or no rise of the terrain. This is was already observed in the transects analysis (**Fig. 37** and **39**), suggesting that these inactive branches may soon become active again.

8.5 Volume calculation

Figure 44 *Chabestan 2017 OrthoMosaic and polygon drawn in PhotoScan*

8.5.1 Chabestan

Differently from what has been done by Hemmelder et al. (2018) in their research, in this research project the calculation of the difference in volume of the whole catchment has been attempted. The selected area extends for 0.21 Km^2 and was traced out of the 2017 OrthoMosaic, as its extent is inferior to the 2016 dataset.

The author opted for setting an ideal reference plane created automatically by PhotoScan according to the position of the vertices. The 2016 catchment has an estimated volume of 924.229 m^3, 97.174 m^3 of which are solely the river area. On the other hand, the 2017 catchment has an estimated volume of 979.076 m^3, with 59.153 m^3 in the river area.

These values suggest a loss of material in the river area and an increase in the vegetation volume in the whole catchment. Yet, this increase in vegetation is not clearly visible from the OrthoMosaic, suggesting that this method has great inaccuracy when it comes to estimating the volume of a highly dense canopy area. On the other hand, the values returned for the river area only might be more truthful as the river area only clearly went through changes and the loss of some vegetation in the southern part of the catchment might explain this difference between 2016 and 2017.

Table 7 *Volume change in Chabestan river area, 2016-2017 (PhotoScan tool method, all values in m^3)*

Total volume	2016	2017
Whole area, no human infrastructure	924.229	979.076
River area only	97.174	59.153
Difference in total volume	**2016-2017**	
Whole area, no human infrastructure	54.847	
River area only	-38,021	

But how this method compares to a more reliable and widespread used method, that is the Cut/Fill tool in ArcGIS? The answer is that they return two (almost) completely different results. In fact, this second method returns lower values compared to the PhotoScan tool but, at least for 2016-2017 (which are the only two comparable years between the two methods), it shows a consistent pattern of volume loss. The only data comparable between the two methods is the difference in total volume, because the Cut/Fill tool works with different inputs than the PhotoScan tool. Therefore, according to this method there is a loss in volume between 2016 and 2017 of 17.300 m^3 of material.

However, this method is of interest because the author was able to calculate the difference of all the DEMs available to him, therefore including the DEMs created by Hemmelder for 2014 and 2015. Of notice is constant loss of material over the years but also a growth of the material gained despite the loss, suggesting that the disruptive events gained strength over the years.

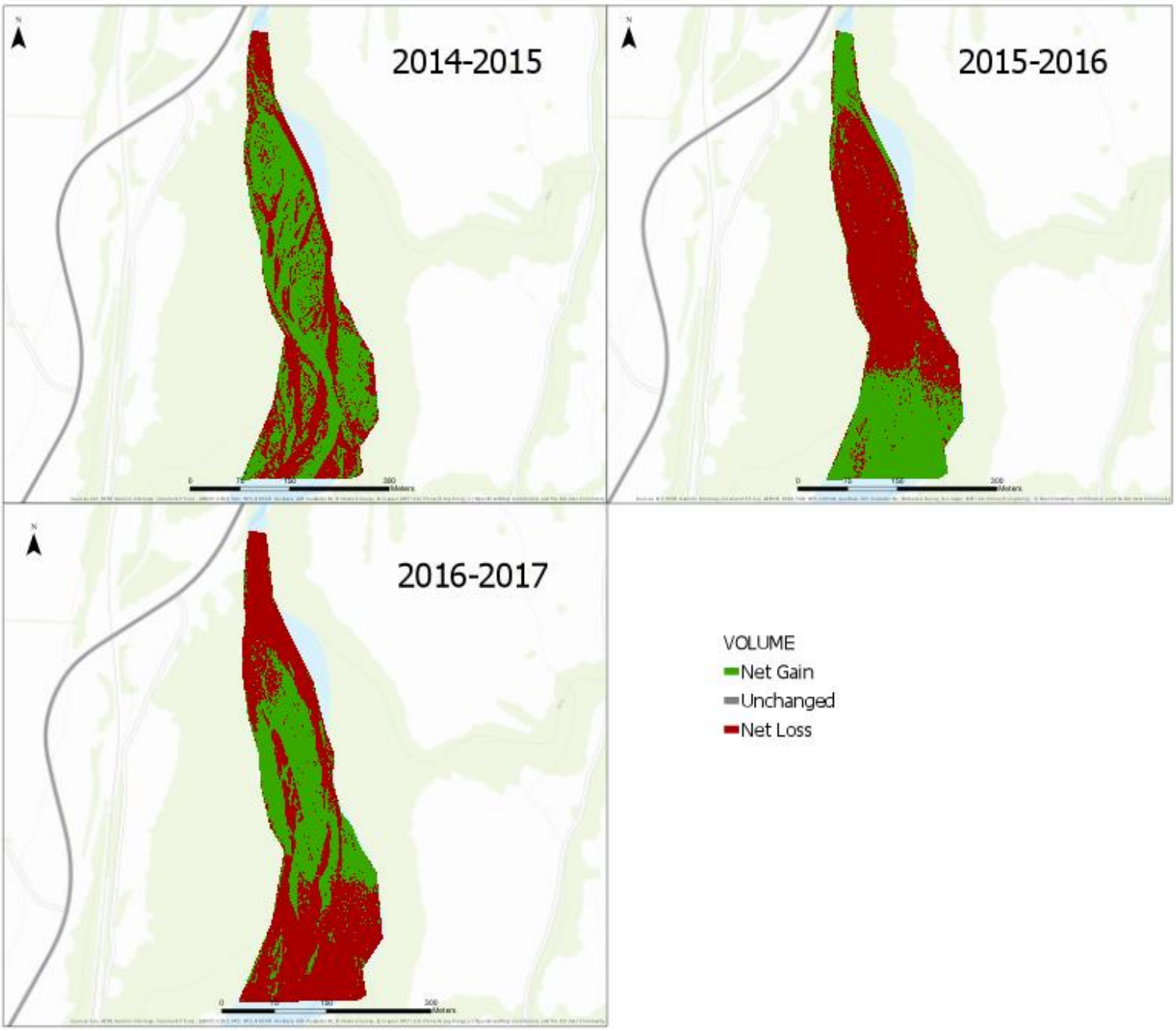

Figure 45 *Volume change time series maps in Chabestan, 2014-2017*

Table 8 *Volume change in Chabestan river area, 2014-2017 (Cut/Fill method)*

	2014-2015	2015-2016	2016-2017
Net Gain (m^3)	10.182	15.007	14.082
Unchanged (m^2)	8	9	2
Net Loss (m^3)	21.228	17.771	31.382
Change in Volume (m^3)	-11.046	-2.764	-17.300

Figure 46 *La Bâtie-Montsaléon 2017 OrthoMosaic and polygon drawn in PhotoScan*

8.5.2 La Bâtie-Montsaléon

As for Chabestan, the selected area was traced out of the 2017 OrthoMosaic. It extends for 0.16 Km^2, the difference with Chabestan resides in the fact that La Bâtie-Montsaléon is surrounded by more fields than woods, that have been left out of the volume calculation as not interesting for purpose of this study.

The same tool and settings, as for Chabestan, were chosen to estimate the volume of this catchment. The total volume estimated for 2016 is 690.223 m^3 while the 2017 estimation is 828.931 m^3. The suggested increase is surprising because the catchment undergoes two clear erosion processes in nearby woodlands. Yet, this catchment shows three different results according to the area analysed. If the whole catchment is considered, including the surrounding woods and excluding the fields and human infrastructure, there is a noticeable increase in the volume. However, if the measurement is made once again with a new polygon drawn only to include the river area of the 2017 OrthoMosaic, this will also include some wooded areas when superimposed on the 2016 OrthoMosaic, giving more insight on were the erosion occurred and where there was a vegetation loss. In fact, these measurement returns a totally different result, with a clear loss of volume from 2016 to 2017. Where the erosion occurred was already visible in the OrthoMosaic comparison (pp 22 and pp 30). Lastly, a measurement on the river area only has been done by drawing a third polygon on the 2016 OrthoMosaic. This returns a small increase over the year, highlighting how the dynamic of this river are much more complex than they look at first sight. If it is true that the vegetation has been eroded and volume has been loss, it is also true that the sedimentation processes were also strong and brought new material in this river area.

Table 9 *Volume change in La Batie-Montsaléon river area, 2016-2017 (PhotoScan tool method, all values in m^3)*

Total volume	2016	2017
Whole area, no human infrastructure	690.223	828.931
Partial vegetation area included	136.824	83.434
Only river area	48.206	49.537
Difference in total volume	**2016-2017**	
Whole area, no human infrastructure	138.708	
Partial vegetation area included	-53.390	
Only river area	1.151	

Differently from the Chabestan study area, La Bâtie-Montsaléon results of the Cut/Fill tool show significant discrepancies between the two methods. The PhotoScan tool method returned a modest increase in volume, while the Cut/Fill method registered a negative loss of -34.401 m^3. In the author opinion, according also to the visual comparison of the OrthoMosaic and the transect analysis, the result yielded by the Cut/Fill tool is more reliable and support the hypothesis that, as for Chabestan, the disruptive events got stronger over the years, but with the difference that while the material gained kept diminishing the material lost increased exponentially.

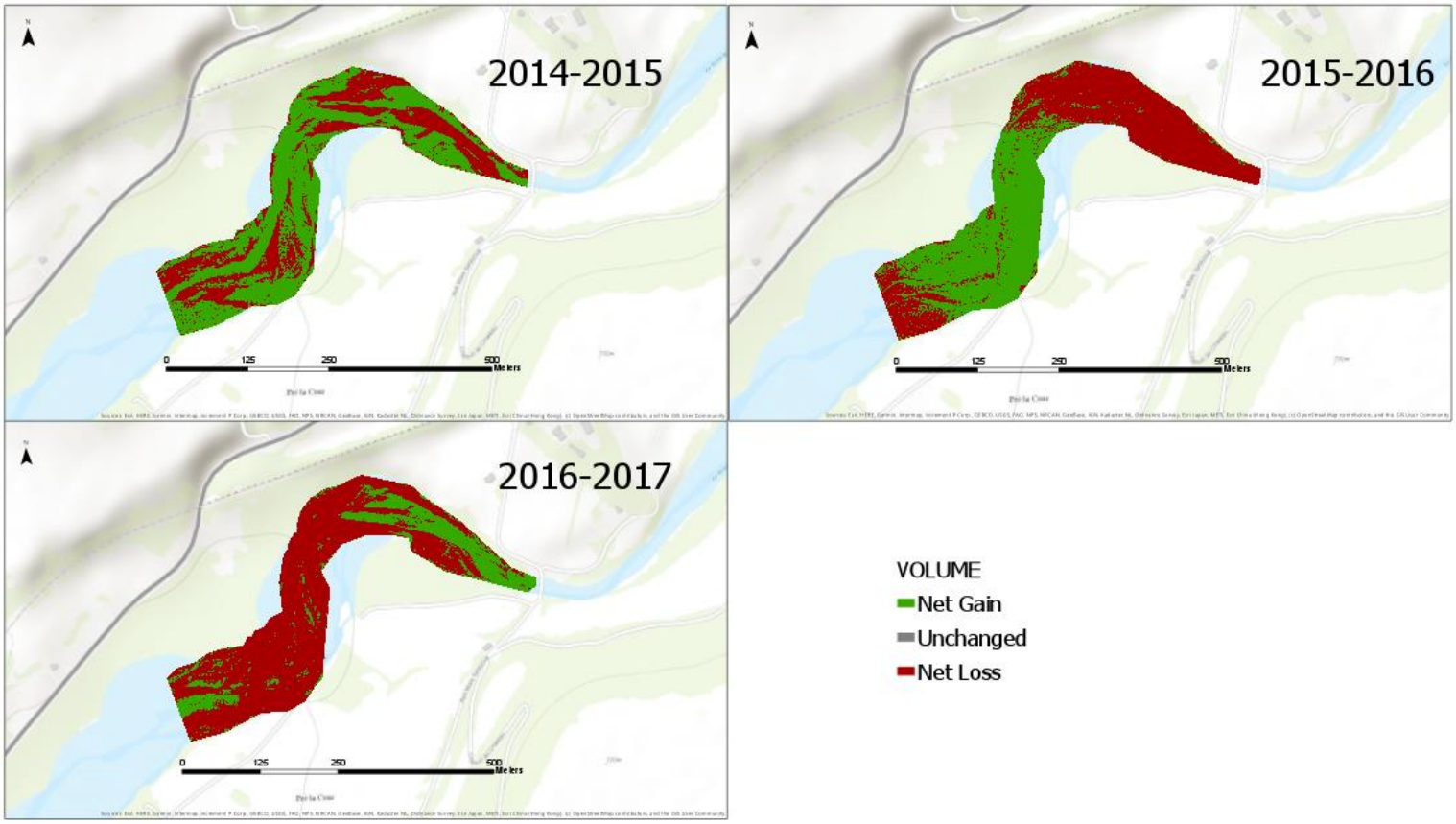

Figure 47 *Volume change time series maps in La Bâtie-Montsaléon, 2014-2017*

Table 10 *Volume Change in La Batie-Montsaléon, 2014-2017 (Cut/Fill method)*

	2014-2015	2015-2016	2016-2017
Net Gain (m^3)	16.569	10.610	10.217
Unchanged (m^2)	5	4	2
Net Loss (m^3)	13.369	18.759	44.618
Change in Volume (m^3)	3.200	-8.149	-34.401

9 Discussion

In this section the results obtained will be discussed obtained and various issues raised during these months of work on the research project will be tackled. Firstly, it will be the more technical aspects of the project, discussing the quality of the final product compared to initial expectations, what can be defined the "source of uncertainties" and finally the changes in the river area.

The first two research subquestions regarded the efficiency of the PhotoScan approach and the ***quality of the final product***. Starting from the latter, it must be pointed out that the expected output of the processed dataset, at the start of this research project, were the following:

- Two OrthoMosaics for the river sections studied, at a precision in the order of ~5 cm;
- The derived DEMs, at a precision of ~10 cm;

The quality of the results were beyond expectations, as the resolution of each product is not worse than 3.36 cm. Both DEM have a higher resolution than the OrthoMosaic, this since the mosaic loses some quality when merging photos with low overlap and fewer key points in common. Moreover, the exceptional quality might be a "double edge sword": while enhancing the possibility of a higher quality analysis on the DEM, it also brings some issues with the OrthoMosaic. In fact, the ultra-high quality of the final mosaic might be considered pointless from a purely aesthetic point of view, as zooming in will reveal the lower quality of the imagery. Besides, the DEM and OrthoMosaics present a lot of holes, hindering on one hand the quantitative analysis of the first and, on the other hand, the visual quality of the second.

Yet, the sources of uncertainties in this project were multiple. Starting from the dataset, the main source of uncertainty was the quality of the imagery available. A lot of photo were cut in the first quality control (for example over 500 photos out of approximately 1600 were cut from the 2016 dataset) because of the very low quality (e.g. blurred, **Fig. 48** left) or because useless to the creation of the products (e.g. test photos taken before the flight, **Fig. 48** right).

Figure 48 *Two examples of discarded imagery, too blurred or before the capture flight*

Yet, some low-quality imagery had to be used anyway. One of the main problems with large catchments like these is having a good overlap of each photo. When this is missing, the program will leave holes in the DEM and mosaic, no matter the photo used is 50 dpi or 500 dpi. Moreover, a lot of photos that had a good quality in terms of stability and lighting were discarded because the program couldn't align them, mainly photos of only the forest surrounding the river (**Figure 49**). This is the main reason of the numerous holes in the forest areas and can be explained by the fact that probably the leaves were moved by the wind, changing position from photo to photo. This made the alignment of this area harder and resulted in a lot of points in the point clouds that needed to be cleaned in order to avoid outliers in the height values.

The problem with the quality of the imagery doesn't end at the blurred photos but further expand if considering the brightness differences. In this project, brightness differences can be observed in two ways: the actual divergence between darker vegetation and the whiteness of the river banks; the presence of photos with different lighting due to clouds. The ideal condition, in photogrammetry, to take photos is in late spring during a

cloudy day at noon (possibly in absence of wind too). This allows the light to be uniform on every object and reducing the reflectance of surfaces like water and the white gravel. Yet, this ideal condition wasn't the condition at the time of the flights, apart from one day in the 2016 dataset. A lot of photos have different lighting and present cloud shadows on the area or bright reflection from the ground and water (**Figure 50**), hindering the alignment, the marker positioning and therefore lowering the quality of the final products. Besides, the water and vegetation are in constant movement because of the natural flow or wind, causing further problems to the SfM algorithm in the alignment phase.

Figure 49 *Example of a decent quality photo not usable as the program couldn't align it and find common key points, even with the presence of a still feature as the train tracks*

Therefore, ***how efficient is the PhotoScan workflow for 3D reconstruction and DEM creation?*** Depending on the task, resources and time available, this workflow might or might not be the right answer. However, this research project showed how the use of this workflow is particularly feasible for academic research projects as well as low budget photogrammetry project. It is simple to understand and the learning curve of the programme is not steep, allowing the user to obtain quite good outputs even after the first run. The issues regarding this workflow will be discussed more extensively in the next chapter, but it is safe to say that PhotoScan and SfM have a proven workflow for studying dynamic environments (Brunier et al., 2016; Eltner et al., 2016; Smith et al., 2015).

Figure 50 *Example of imagery with different lighting. This affects the ability of the program to find common points as the sun is too bright or clouds are temporally covering part of the catchment*

Lastly, of note is the importance of the flying path when considering the quality of the imagery. This paragraph will also try to give an answer to the third subquestion, about the ***usefulness of oblique imagery DEM reconstruction***. The UAV utilised for this project is nor a drone-helicopter nor a plane-UAV. It is very cheap compared to what normally is used in photogrammetry and was lacking all the utilities held by classic (and more expensive) UAVs. It didn't have a flight GPS to catch the position of each photo or a pre-programmable flight path and the camera, cheap as well, was manually shot with a remote control. This resulted in varying heights and different scales during the flight. Yet, these are not necessarily bad factors when using PhotoScan and the SfM algorithm, as it is specified in its manual that it can work fine regardless of scale and angle, as long as the program can recognise identical points in the imagery.

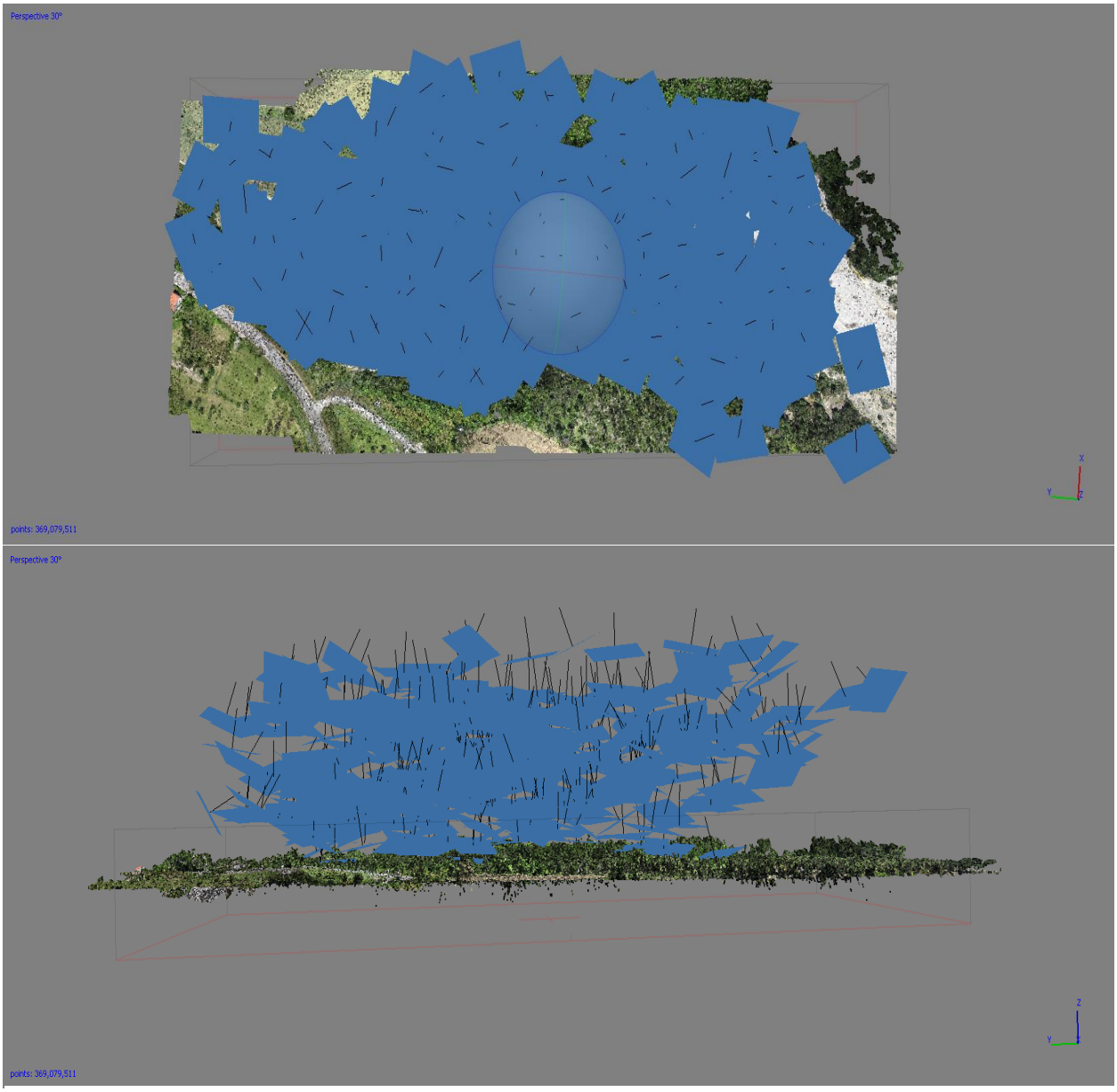

Figure 45 *The camera position for the Chabestan 2017 flights. The randomness and difference in height and angle affect the processing time and quality of the dataset, other than requiring a higher number of photos to achieve a good overlap*

However, the results of the lack of a flying path can be seen in the previous page (**Fig. 45**) and below (**Fig. 46**). Above we can see how the photos are taken in random position, heights and angles. As said, this is not necessarily a problem for the program, however, minimize the difference in scale, height and angles of the photos taken will assure a higher quality product in the end (Chandler, Ashmore, Paola, Gooch, & Varkaris, 2002). Below, the two figures perfectly exemplify the need of a coherent flight: the two photos have a very low angle of shooting and the result are these "panoramic" shoots of the river. The problem in this case is not the alignment, as the quality

of the photos is good and will be a good source for the final OrthoMosaic, but the impossibility to locate with precision all the markers on the ground. The green flag are the markers manually positioned, while the grey symbol represents the location estimated by the program, which is not necessarily accurate and therefore enhancing the uncertainty and location error of all the other markers in the next alignments.

Yet, in absence of GCPs and camera parameters, the addition of oblique imagery to the reference dataset is proven to diminish DEM deformation and a reduction on the error of the estimated parameters (James, Robson, d'Oleire-Oltmanns, & Niethammer, 2017). Moreover, oblique imagery is demonstrated to be effective when the study area present high cliffs and steeps, yielding a product that will return more accurate result for advanced analysis such as estimation of sediment transported and flow data modelling (Chandler et al., 2002).

Figure 46 *Two examples of decent quality resolution imagery, but bad angles of shooting. The markers in the end of the catchment are impossible to manually locate, returning higher uncertainty and a less accurate alignment*

9.1 River behaviour

The second set of research questions posed for this project were regarding **the behaviour of the river**. As follows a recap of the subquestions and a discussion on what the findings tell us about the river behaviour:

- **Is there any change in the morphology of the river between 2016 and 2017?**
- **If any, is it stronger than previous years?**
- **Is it a threat to human activity?**
- **Is the river area subjected to mass soil loss and, if so, is it quantifiable?**

The analysis on the products yielded showed how the Buëch river has high dynamism and undergoes great transformation between the years, proving to be a potential threat for human activity and infrastructure.

The slope map and the transect analysis showed high levels of sedimentation, possibly associated with the few but strong high discharge events that occur during the year. The volume analysis with the Cut/Fill tool sustains this proposition.

At La Bâtie-Montsaléon a large wooden area has been eroded, with consequent loss of volume of about 3000 m^3. This eroded area show continuance with the findings of Hemmelder et al. (2018), where from 2014 and 2015 the same location saw heavy erosion in the same direction and with the same intensity. As for his study, it is not possible to find direct data on the discharge events that caused this massive erosion episodes, therefore it is unpredictable when and where the next will occur. Yet, the results of Hemmelder et al. (2018) research and the present research can be related to obtain a timeseries that shows certain trends in the river dynamics allowing future studies to understand if there is an erosion pattern in certain locations, as for La Bâtie-Montsaléon specifically.

The Hautes-Alpes region saw an afforestation process on its slopes in the last decades, associated to the abandonment of these areas but also thanks to the successful correction of torrential watersheds by the

Restoration of the Lands in Mountain (Restauration de Terrains en Montagne). Consequently, the quantities of sediments injected by the torrents into the three branches of the Buëch have certainly decreased significantly in the course of the 20th century due to the alleviation of erosive processes on the slopes (Gautier, 1994).

Nevertheless, the Petit Buëch showed, over the last five years, a constant change in its river bank (Hemmelder et al., 2018), closing the gap with human settlements and roads, eroding agricultural land and laying the foundations for serious issues with the nearby train line. As river bank erosion might have an impact on these agricultural catchments, on the other hand, it must be considered the impact of this activities on the surrounding environment. The extraction of aggregates has been a common practice in the Buëch catchment area (Gautier, 1994). This had a huge impact on the river's dynamics, reflected in the local incision of the river bed, but also by regressive and progressive erosions that implicate a lowering of the river bed (Bravard et al., 1999). Channel displacement is another consequence of these intense discharge events.

The present research showed how the channel changes its path greatly during the year and the use of timeseries maps will allow to identify precisely the active and, especially, inactive channels. This will result in more predictable changes and allows a deeper analysis on the causes and effects of these changes, other than give more insight on the dynamics of the Buëch river. Yet, what is missing or, at least, what needs to be improved in the author's opinion is a solid volume calculation method. The two methods used returned different absolute values and the measurement by using the tools in PhotoScan are still unreliable for an accurate volume calculation. Yet, even though the area analysed were different (the Cut/Fill tool in ArcGIS used the full DEMs) and the values very dissimilar, it is possible to see similar trending pattern in growth or decrease in volume. However, the author doesn't recommend the use of PhotoScan only for measurement and suggests the use of more suited program such as ArcGIS to deal with volume calculations.

9.2 Issues

The results obtained through this research showed how the potential of PhotoScan in processing numerous aerial photographs at Ultra-High quality. Yet, various problems and challenges arose during these months of work. In this section will be highlighted the most significant challenges and issues the author had to tackle to successfully finish this research project and the personal suggestions on how to improve or avoid these situations in future research.

9.2.1 Reference system

The biggest problem encountered in this research project was the difference of the reference system between the 2017 dataset and all the others. The dataset between 2014 and 2016 all shared the same coordinate system, "WGS 84/UTM zone 31 N", while the latest dataset available was projected in a local French projection, RGF 1993 Lambert 93. The difference was known from the start, but issues started to arise when analysing and comparing the 2016 DEM with the reprojected 2017 DEM. The Z values of the latter where different from all the other datasets and the model resulted to be located on different reference plane, about 50 m below the dataset from 2014 to 2016. This is noticeable in the transect analysis.

Although the above-mentioned difference in reference system was acknowledged since the start of this research project, the results returned unexpected outputs. The 2017 dataset, in fact, seemed to lie on a different reference height plane. The difference in height values, as said, was already known and deemed to be caused by the different coordinate system. Yet, the conversion in the PhotoScan or ArcGIS didn't yield the expected results.

The models are not erroneous per se and are possible to compare, both the volume and bank displacement. This difference is not hindering the analysis and comparison of the datasets, because the XY values are correct and PhotoScan cleverly run the volume measurement or profile drawings directly on a reference plane custom created for each model. However, this raises questions on why the 2017 dataset was incorrect and what could have been done to fix it. First of all, the 2017 Z values are actually correct and the other dataset were wrongly converted. This is possible to check in different ways: on the Utrecht University drives there is an official, coarse, DEM of France, where the height values of fixed location are much closer to the Z values of the 2017 dataset (716 m in the DEM, 721 m in 2017, 753 m in 2014-2016). Similar values are found on official topographic maps on the French geoportal in the surrounding areas (**Fig. 52**). Also, other unofficial sources such as Google Earth and Wikipedia suggest that the correct height values of the area are the ones found in the 2017 dataset.

Figure 51 *Highlight from the official topographic map of France on their geoportal (height values in the red circle). The values showed are from surrounding areas of the river*

Therefore, what happened? The author opinion is that there was simply an error in the conversion of the raw DGPS data of the markers to the final output given to him. Most probably the wrong vertical datum in the Lambert to UTM conversion that was done, leading to this misrepresentation of the data on different reference plane.

Nevertheless, this brought a new unexpected challenge. In fact, the error relies in the original .csv file, with the marker's coordinates, that was provided at the start of this research project. Three possible solutions were thought to deal with this issue: (1) a new conversion of the raw coordinates, trying to fix the original Z values of the 2017 to be able to homogenously compare it with the other dataset. This is not ideal because the final height value would be incorrect, and it would be best to reconvert all the other datasets. Clearly, this was not possible to accomplish for time and scope constraints. (2) a systematic shift of the datasets to the correct height. This is not ideal, as a systematic shift of the reference plane is prone to errors, but at the same time the fastest way to deal with the problem and allowing more accurate volume calculation in ArcGIS. (3) no change, the error is acknowledged and dealt the best way possible. The analysis in PhotoScan is still possible, the transect profile analysis doesn't undergo changes even when the model is reprojected in wrong coordinates system on purpose. Same applies to the volume change, as the reference plane created by PhotoScan is based on the model 3D model itself, minimizing the problems with the Z values.

A blend solution of the latter two was followed, by shifting the 2017 dataset to the wrong reference plain for comparison sake but acknowledging the error and keeping the 3D model at the same height for the analysis in PhotoScan.

9.2.2 PhotoScan processing time

PhotoScan proved to be an excellent program to work with UAV imagery. The main advantages and disadvantages of UAV photogrammetry have been already pointed out (pp 23-24), same for the reasons

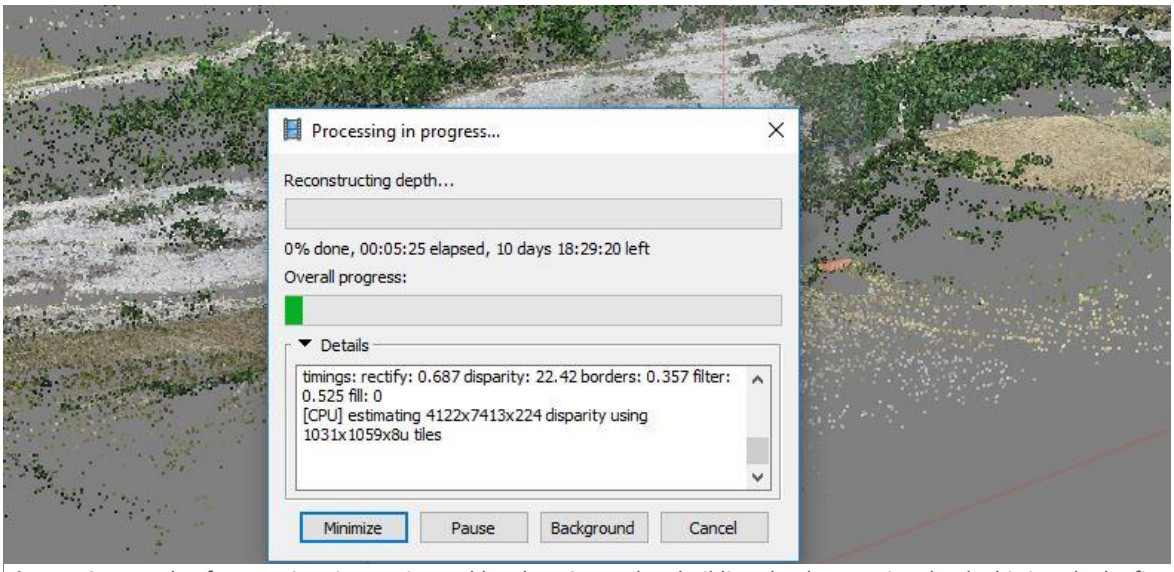

Figure 52 *Example of processing time estimated by PhotoScan when building the dense point cloud. This is only the first step the program takes when building the whole point cloud, in the end the process should take about 10/11 days if run only on one computer and aiming for ultra-high-quality*

Photoscan has been used. Still, a small digression on the weak aspects of the program must be done. Photoscan is a beautiful tool to work with, as it is simple to learn to use and quite straightforward in presenting a smooth and clean workflow to follow. Besides, the program as a lot of online support and finding solutions to rising problems is generally simple.

Nevertheless, it has some flaws. The main drawback is possibly the length of the dense point cloud. Processing the dataset to obtain Ultra-High outputs is incredibly time consuming if done with only one computer and the requirements to run processes at that resolution will require very powerful computers. In order to obtain a textured 3D model with relative DEM and OrthoMosaic out of a dataset of 350 photos, the process will take up to a full week of continuous processing. Trying to run a process with all 850 photos (as for Chabestan 2017) will fail, but this is not a problem as PhotoScan overcome the problem by allowing the creation of multiple batches that can be merged in the end.

The ideal solutions to this processing issue are two, one “offered” by PhotoScan itself and another that relies on cloud computing. PhotoScan allows the users not only to separate in different batches the dataset, but also give the possibility to network the process with other computers. Besides the great potential given, this is still a drawback in the author’s opinion. To run the network processing the user needs to be in possession of other Photoscan licenses, which are not cheap, and capable computers to run the process. This translates in a cost-ineffective methodology, that counters all the economic advantages of UAV photogrammetry.

9.2.3 Overhanging vegetation

The output yielded by the program, as seen before (insert page number), are of extremely high resolution. However, as already pointed out by Hemmelder et al. (2018), the products yielded are DSM and not DTM. In general, DSM are not well suited for bank erosion analysis compared to DTM, as the latter gives elevation data to the ground and not also of the vegetation canopy. This becomes problematic when the vegetation overhangs on the channel banks (Brunier et al., 2016), invalidating part of the analysis in certain locations. Moreover, the problem with overhanging vegetation is not just an issue with the output results, but also when trying to locate the markers on the aerial photos. This is an issue that can’t be directly controlled but there are solutions to overcome this major issue, like planning a flight path.

The issue was already addressed by Hemmelder et al. (2018) and yet is and will be a major challenge when studying these areas. The overhanging vegetation not only makes harder to estimate the erosion of the banks

but also blurs on its edges in the OrthoMosaic, making the determination of the river banks even harder. Clearly, this is the main disadvantage when comparing photogrammetry products with Lidar products.

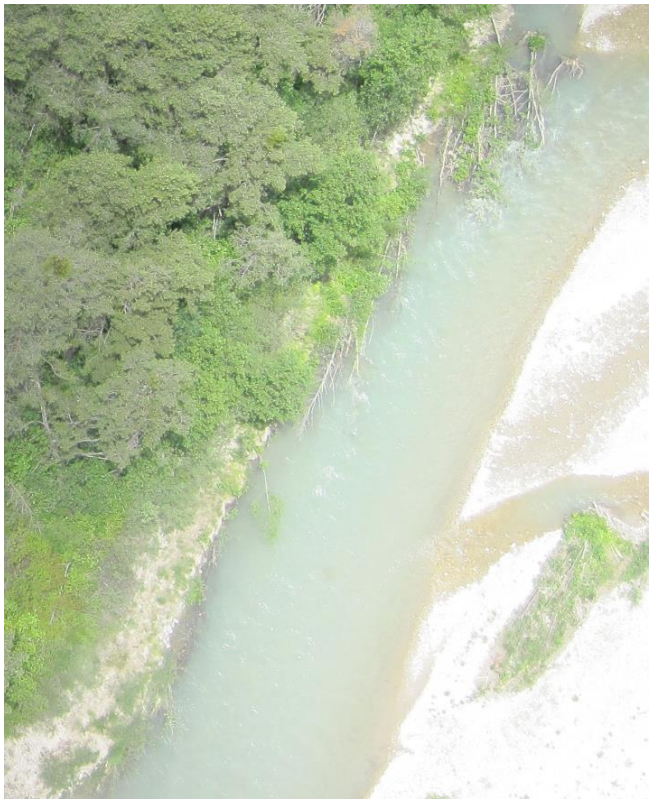

Figure 53 *Two examples of overhanging vegetation that make hard locating the banks, estimating their erosion and place the markers on the photos*

9.2.4 Classification channel displacement

Differently from Hemmelder et al. (2018), to classify the channel displacement it has not been used any type of automatic classification. The result given by supervised and unsupervised classification were inconsistent and the river channel was always selected with part of the surrounding areas, especially when close to vegetation. Also, the selection tools present in graphical programs such as Paint 3D and Adobe Photoshop proved to be inconsistent as large part of vegetation where selected. The solution opted by the author, in the end, was to manually digitize the river banks. The result is less precise and clearly other classification methods would be preferred, but for the type of analysis done and time available, this was the most efficient method.

9.3 Recommendations

To overcome these issues and obtain even higher quality results the author suggests some changes in the data acquisition.

The ideal would be having a drone with a camera integrated with all the tools necessary to record camera position and altitude.Since this research project demonstrated that it is possible to achieve extremely high-quality results with a cheap drone and camera, it is not necessary to change the UAV, but an integration of the above-mentioned tools would enhance significantly the results and reducing processing times (Smith et al., 2015).

Last generation UAVs come also with possibility to plan automatically the flight path and set the camera to automatically shoot. A lot of photos in the dataset available have an overall bad quality but good enough to yield Ultra-High resolution DEMs and OrthoMosaics. Planning a flight path would allow to have access to a coherent set of photos that have an identical shooting angle and a better overlap. The result will be a smaller dataset but of higher quality imagery, greatly reducing the processing time (as photos are compared in clusters and not one by one) and enhancing the final quality.

10 Conclusions

This research project proved to yield positive results. The use of cheap tools to capture the imagery didn't affect the final quality of the end product. Agisoft PhotoScan workflow proved to be well suited for the task and yielded results with quality exceeding initial expectations. It has some flaws (e.g. time-consuming processes) but workarounds (e.g. CPUs cluster network) can be applied to overcome them and end with an ultra-high quality product.

Here the author will draw the conclusions and give a final answer to the research questions posed at the start of this research project.

- **How the creation of a DEM, the related OrthoPhoto and 3D model can help with river bank analysis?**
    - Is 'Agisoft PhotoScan' workflow the best approach for 3D mapping and DEM construction?
    - What is the quality and accuracy of the obtained products?
    - Does using oblique images raise any problem in data processing or may be an advantage for the resulting 3D model?

Agisoft PhotoScan proved to be a worthy program for ultra-high quality 3D mapping and DEM construction from drone imagery. If 3D mapping is still far away from being an accurate and efficient source for morphological analysis, the OrthoMosaics and DEMs yielded by Photoscan are impressive. The achievable resolution is incredible and the learning curve of the program is not steep, giving the possibility to produce high quality product even with limited photogrammetry knowledge. The workflow is clear and easy to follow, yet PhotoScan is recommended to be used only for building the point clouds and the derived OrthoMosaics and DEMs. For more complex measurement or analysis other programs are better suited for the task, such as CloudCompare for the point cloud analysis and ArcGIS for the volume measurements.

As said, the quality of the yielded product is phenomenal, with the coarsest product having 0.36 cm of resolution. Moreover, the positional accuracy of each product is incredibly high, with an error of the ground control points of 0.25 m on average, but with an enormous difference between the two years (e.g. at La Batie-Montsaléon the error is 0.68 m in 2016 and 0.03 m in 2017).

One of the reasons of this discrepancy is the oblique imagery taken by the UAV. The use oblique imagery is not harmful for recreating the 3D model of the study area and the subsequent OrthoMosaic and DEM. PhotoScan deals pretty well with oblique imagery and has no problem in aligning the oblique photos for model building. Actually, the use of oblique imagery in an area like the one studied in this research project could have been helpful, as the reconstruction of the banks closer to the vegetated area is quite hard because of the overhanging vegetation. In addition, oblique imagery is a good source for texturing the 3D model. However, oblique imagery could also be harmful if not taken with care and might give problems, like hindering the manual positioning of the GCPs and therefore the creation of the sparse point cloud. To avoid any problem with oblique imagery, the easiest and best solution is to use drone with stabilizer and a planned automated flight path. This will ensure minimal noise in the picture as well as a homogeneous dataset to work with.

This research project had also a second focus, analysing the river area morphology and dynamics through the use of the above mention photogrammetric techniques. Below the research questions posed at the start of this research.

- **What is the behaviour of the river bank?**
    - Is there any change in the morphology of the river between 2016 and 2017?
    - If any, is it stronger than previous years?
    - Is it a threat to human activity?

- Is the river area subjected to mass soil loss and, if so, is it quantifiable?

The behaviour of the riverbank resulted to be almost unpredictable, as expected in a dynamic system such as a braided river. Changes in the morphology are clearly visible thanks to the high quality of the imagery, that allows to do a visual comparison of the OrthoMosaics, analysing channel displacement and bank erosion. An eroding pattern has been noticed in certain areas of La Bâtie-Montsaléon, giving great importance to future similar research in the area. These findings were already present in Hemmelder et al. (2018) work and confirmed again in the present report. Moreover, the DEMs analysis showed, once again, the high dynamism of the river and the constant change in volume of the area. In the Chabestan area both methods used to estimate volume change share a similar pattern, with a loss of material in the river area between 17.000 m^3 (ArcGIS measurement) and 38.000 m^3 (PhotoScan measurement). Different the results yielded in the La Batie river area where the PhotoScan measurement registered a small gain of just about 1100 m^3 while the measurement in ArcGIS show a great loss of about 34.000 m^3.

The lack of data on destructive flooding events makes hard to predict when and where the next heavy erosion processes will occur in the area. The terrain next to the railway and the bridges in both catchments saw a constant erosion that might cause major problem soon. The presence of inactive or semi-active channels in the southern part of the catchment at La Bâtie-Montsaléon are also of potential worrying, as the erosion process is persistent over the years and will enhance the risk of major flooding of this flat agricultural area.

Lastly, the river is subject to mass soil loss but, rather more, it is subject to a loss of vegetation. Yet, as pointed out in the results chapter, quantifying this loss is hard to prove and compare over the years, in the author's opinion, as the lack of reference data leave the volume analysis questionable and with the need of further research in the area.

To conclude, this research project is meant to have a follow up and expansion of the current time series. Recommendations on how to capture better quality imagery have been given in the previous chapter and particular emphasis is placed on having a coherent coordinate system to avoid any problems with the analysis and comparison of the data.

11 References

11.1 Bibliography

Agisoft. (2018). Agisoft PhotoScan User Manual: Professional Edition, Version 1.4. *Professional Edition, Version 1.4*, 37. Retrieved from http://www.agisoft.com/pdf/photoscan-pro_1_1_en.pdf

Aicardi, I., Chiabrando, F., Grasso, N., Lingua, A. M., Noardo, F., & Spanó, A. (2016). UAV photogrammetry with oblique images: First analysis on data acquisition and processing. *International Archives of the Photogrammetry, Remote Sensing and Spatial Information Sciences - ISPRS Archives*, *2016–Janua*, 835–842. https://doi.org/10.5194/isprsarchives-XLI-B1-835-2016

Akhtar, M. P., Sharma, N. A. Y. A. N., & Ojha, C. S. P. (2011). Braiding process and bank erosion in the Brahmaputra River. *International Journal of Sediment Research*, *26*(4), 431–444. https://doi.org/10.1016/S1001-6279(12)60003-1

Barbero, M., & Chappaz, M. (2010). *Le Buech*.

Bravard, J. P., Landon, N., Peiry, J. L., & Piégay, H. (1999). Principles of engineering geomorphology for managing channel erosion and bedload transport, examples from French rivers. *Geomorphology*, *31*(1–4), 291–311. https://doi.org/10.1016/S0169-555X(99)00091-4

Bristow, C. S., & Best, J. L. (1993). Braided rivers: perspectives and problems. *Geological Society, London, Special Publications*, *75*(1), 1–11. https://doi.org/10.1144/GSL.SP.1993.075.01.01

Brocard, G. Y., van der Beek, P. A., Bourlès, D. L., Siame, L. L., & Mugnier, J. L. (2003). Long-term fluvial incision rates and postglacial river relaxation time in the French Western Alps from10Be dating of alluvial terraces with assessment of inheritance, soil development and wind ablation effects. *Earth and Planetary Science Letters*, *209*(1–2), 197–214. https://doi.org/10.1016/S0012-821X(03)00031-1

Brunier, G., Fleury, J., Anthony, E. J., Pothin, V., Vella, C., Dussouillez, P., … Michaud, E. (2016). Application de la technique de photogrammétrie Structure-from-Motion pour des levés haute résolution en géomorphologie côtière et fluvial. *Geomorphologie: Relief, Processus, Environnement*, *22*(2), 147–161. https://doi.org/10.4000/geomorphologie.11358

Chandler, J., Ashmore, P., Paola, C., Gooch, M., & Varkaris, F. (2002). Monitoring river channel change using terrestial oblique digital imagery and automated digital photogrammetry.

Charlton, R. (2007). *Fundamentals of fluvial geomorphology / Ro Charlton*. *Sedimentation Engineering*. https://doi.org/10.1111/j.1475-4762.2009.883_5.x

Cook, K. L. (2017). An evaluation of the effectiveness of low-cost UAVs and structure from motion for geomorphic change detection. *Geomorphology*, *278*, 195–208. https://doi.org/10.1016/j.geomorph.2016.11.009

Diaz-Varela, R. A., Zarco-Tejada, P. J., Angileri, V., & Loudjani, P. (2014). Automatic identification of agricultural terraces through object-oriented analysis of very high resolution DSMs and multispectral imagery obtained from an unmanned aerial vehicle. *Journal of Environmental Management*, *134*, 117–126. https://doi.org/10.1016/j.jenvman.2014.01.006

Dietrich, J. T. (2016). Riverscape mapping with helicopter-based Structure-from-Motion photogrammetry. *Geomorphology*, *252*, 144–157. https://doi.org/10.1016/j.geomorph.2015.05.008

Downs, P. W., & Simon, A. (2001). Fluvial geomorphological analysis of the recruitment of large woody debris in the Yalobusha river network, Central Mississippi, USA. *Geomorphology*, *37*(1–2), 65–91. https://doi.org/10.1016/S0169-555X(00)00063-5

Eltner, A., Kaiser, A., Castillo, C., Rock, G., Neugirg, F., & Abellán, A. (2016). Image-based surface reconstruction

in geomorphometry-merits, limits and developments. *Earth Surface Dynamics*, *4*(2), 359–389. https://doi.org/10.5194/esurf-4-359-2016

Fonstad, M. A., Dietrich, J. T., Courville, B. C., Jensen, J. L., & Carbonneau, P. E. (2013). Topographic structure from motion: A new development in photogrammetric measurement. *Earth Surface Processes and Landforms*, *38*(4), 421–430. https://doi.org/10.1002/esp.3366

Gautier, E. (1994). Interférence des facteurs anthropiques et naturels dans le processus d'incision sur une rivière alpine - L'exemple du Buëch (Alpes du sud) / Interaction between human and natural factors in the entrenchment of an alpine river - The example of the Buëch Ri. *Revue de Géographie de Lyon*, *69*(1), 57–62. https://doi.org/10.3406/geoca.1994.4238

Gonizzi Barsanti, S., Remondino, F., & Visintini, D. (2013). 3D SURVEYING AND MODELING OF ARCHAEOLOGICAL SITES – SOME CRITICAL ISSUES – *ISPRS Annals of Photogrammetry, Remote Sensing and Spatial Information Sciences*, *II-5/W1*(September), 145–150. https://doi.org/10.5194/isprsannals-II-5-W1-145-2013

Grenzdörffer, G. J., Engel, A., & Teichert, B. (2008). THE PHOTOGRAMMETRIC POTENTIAL OF LOW-COST UAVs IN FORESTRY AND AGRICULTURE. *XXI ISPRS Congress, Commission I*, *XXXVII-B1*(January 2008), 1207–1214. https://doi.org/10.2747/1548-1603.41.4.287

Haarbrink, R. ., & Koers, E. (2006). Helicopter UAV For Photogrammetry And Rapid Response. *The International Achives Photogrammetry, Remote Sensing and Spatial Information Sciences,Antwerp Belgium. Vol XXXVI-I/W44*, *XXXVI*, 2–5.

Hemmelder, S., Marra, W., Markies, H., & De Jong, S. M. (2018). Monitoring river morphology & bank erosion using UAV imagery – A case study of the river Buëch, Hautes-Alpes, France. *International Journal of Applied Earth Observation and Geoinformation*, *73*(July), 428–437. https://doi.org/10.1016/j.jag.2018.07.016

Hugget, R. J. (2007). Fundamentals of Geomorphology. Retrieved from http://journals.sagepub.com/doi/10.1177/0192623310385829

IGN. (2016). *BD Forêt® Version 2.0*.

Irschara, a, & Kaufmann, V. (2010). Towards fully automatic photogrammetric reconstruction using digital images taken from UAVs. *Proceedings of the International Society for Photogrammetry and Remote Sensing*, *XXXVIII*(October 2015), 65–70. Retrieved from http://aerial.icg.tugraz.at/papers/uav_reconstruction_isprs2010.pdf

Irstea, & Conseil Départemental des Hautes-Alpes. (2017). Technical note about the monitoring of hydromorphological restoration of the Upper Drac River (Hautes-Alpes, France), 12. Retrieved from http://www.alpine-space.eu/projects/hymocares/case-studies/buech_technical-reports.pdf

James, M. R., Robson, S., d'Oleire-Oltmanns, S., & Niethammer, U. (2017). Optimising UAV topographic surveys processed with structure-from-motion: Ground control quality, quantity and bundle adjustment. *Geomorphology*, *280*, 51–66. https://doi.org/10.1016/j.geomorph.2016.11.021

Javernick, L., Brasington, J., & Caruso, B. (2014). Modeling the topography of shallow braided rivers using Structure-from-Motion photogrammetry. *Geomorphology*, *213*, 166–182. https://doi.org/10.1016/j.geomorph.2014.01.006

Kršák, B., Blišťan, P., Pauliková, A., Puškárová, P., Kovanič, L., Palková, J., & Zeliznaková, V. (2016). Use of low-cost UAV photogrammetry to analyze the accuracy of a digital elevation model in a case study. *Measurement: Journal of the International Measurement Confederation*, *91*, 276–287. https://doi.org/10.1016/j.measurement.2016.05.028

Lane, E. W. (1957). A Study Of The Shape Of Channels Formed By Natural Streams Flowing In Erodible Material.

Piégay, H., Darby, S. E., Mosselman, E., & Surian, N. (2005). A review of techniques available for delimiting the erodible river corridor: A sustainable approach to managing bank erosion. *River Research and Applications*, *21*(7), 773–789. https://doi.org/10.1002/rra.881

Piégay, H., Grant, G., Nakamura, F., & Trustrum, N. (2006). Braided river management: from assessment of river behaviour to improved sustainable development. *Braided Rivers: Process, Deposits, Ecology and Management. Special Publication No. 36 of the International Association of Sedimentologists.*, 257–310.

Pineux, N., Lisein, J., Swerts, G., Bielders, C. L., Lejeune, P., Colinet, G., & Degré, A. (2017). Can DEM time series produced by UAV be used to quantify diffuse erosion in an agricultural watershed? *Geomorphology*, *280*, 122–136. https://doi.org/10.1016/j.geomorph.2016.12.003

Remondino, F., & Barazzetti, L. (2012). Uav Photogrammetry for Mapping and 3D Modeling – Current Status and Future Perspectives. *ISPRS - International Archives of the Photogrammetry, Remote Sensing and Spatial Information Sciences*, *XXXVIII-1/*(September), 25–31. https://doi.org/10.5194/isprsarchives-XXXVIII-1-C22-25-2011

SDAGE. (2013). Études D'Estimation Des Volumes Prélevables Globaux.

Smith, M. W., Carrivick, J. L., Hooke, J., & Kirkby, M. J. (2014). Reconstructing flash flood magnitudes using "Structure-from-Motion": A rapid assessment tool. *Journal of Hydrology*, *519*(PB), 1914–1927. https://doi.org/10.1016/j.jhydrol.2014.09.078

Smith, M. W., Carrivick, J. L., & Quincey, D. J. (2015). Structure from motion photogrammetry in physical geography. *Progress in Physical Geography*, *40*(2), 247–275. https://doi.org/10.1177/0309133315615805

Summerfield, M. A. (1991). *Global Geomorphology*. *Encyclopedia of geomorphology* (Vol. 1).

The Center for Photogrammetric Training. (n.d.). History Of Photogrammetry. https://doi.org/10.1179/174581607x254776

Westoby, M. J., Brasington, J., Glasser, N. F., Hambrey, M. J., & Reynolds, J. M. (2012). "Structure-from-Motion" photogrammetry: A low-cost, effective tool for geoscience applications. *Geomorphology*, *179*, 300–314. https://doi.org/10.1016/j.geomorph.2012.08.021

Whipple, K. X., Hancock, G. S., & Anderson, R. S. (2000). River incision into bedrock: Mechanics and relative efficacy of plucking, abrasion, and cavitation. *Bulletin of the Geological Society of America*, *112*(3), 490–503. https://doi.org/10.1130/0016-7606(2000)112<490:RIIBMA>2.0.CO

11.2 Websites

https://water.usgs.gov/edu/earthhowmuch.html

https://www.globalforestwatch.org/

http://www.hydro.eaufrance.fr/selection.php

http://desktop.arcgis.com/en/arcmap/10.3/tools/spatial-analyst-toolbox/how-cut-fill-works.htm

12 Appendix

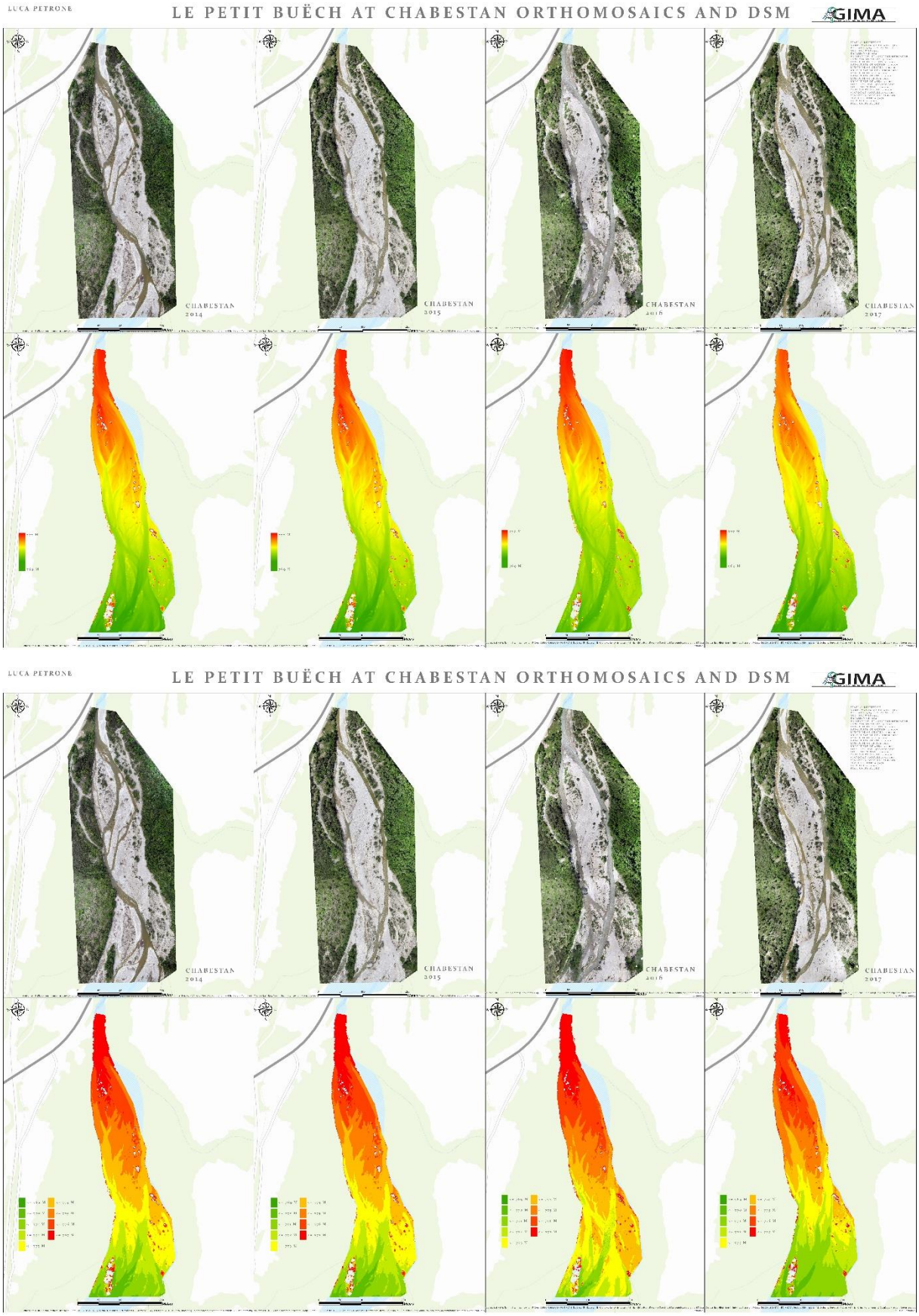

Figure 54 *Chabestan timeseries ("Stretched" and "Classify" classification method)*


LA BÂTIE-MONTSALÉON 2014

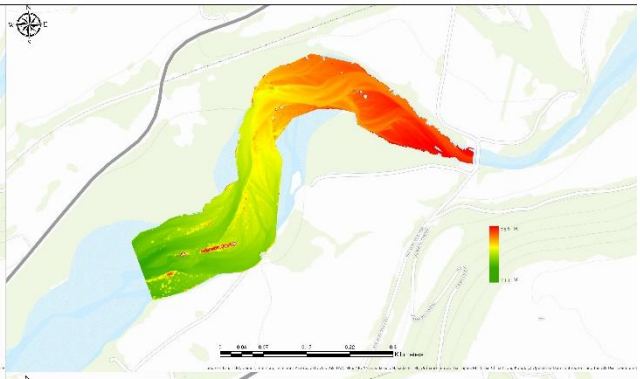


LA BÂTIE-MONTSALÉON 2015

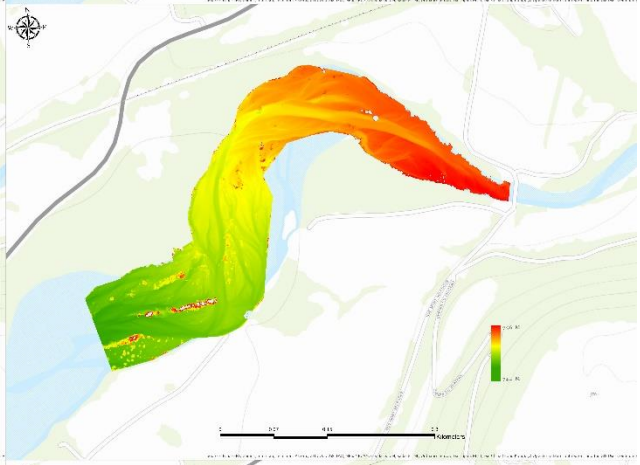


LA BÂTIE-MONTSALÉON 2016

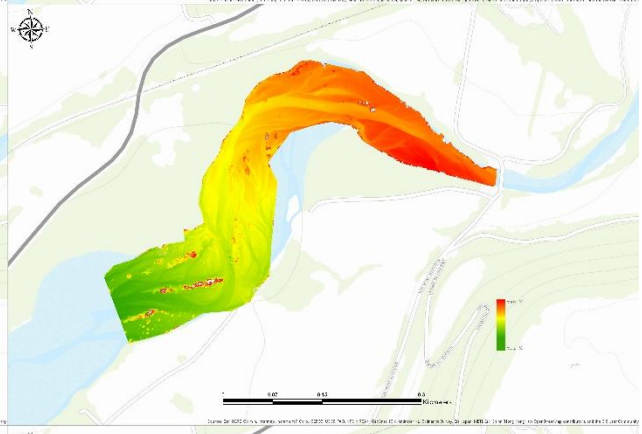


LA BÂTIE-MONTSALÉON 2017

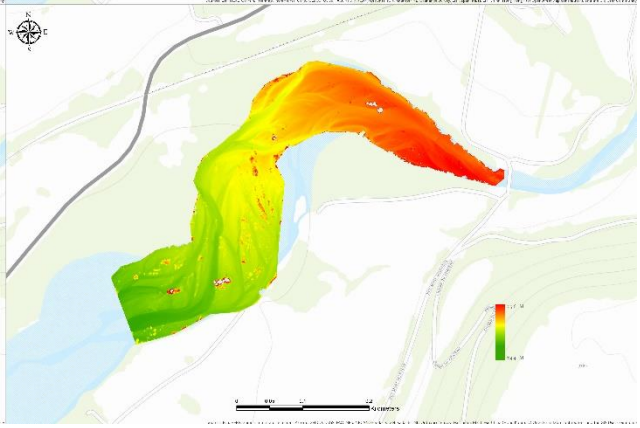

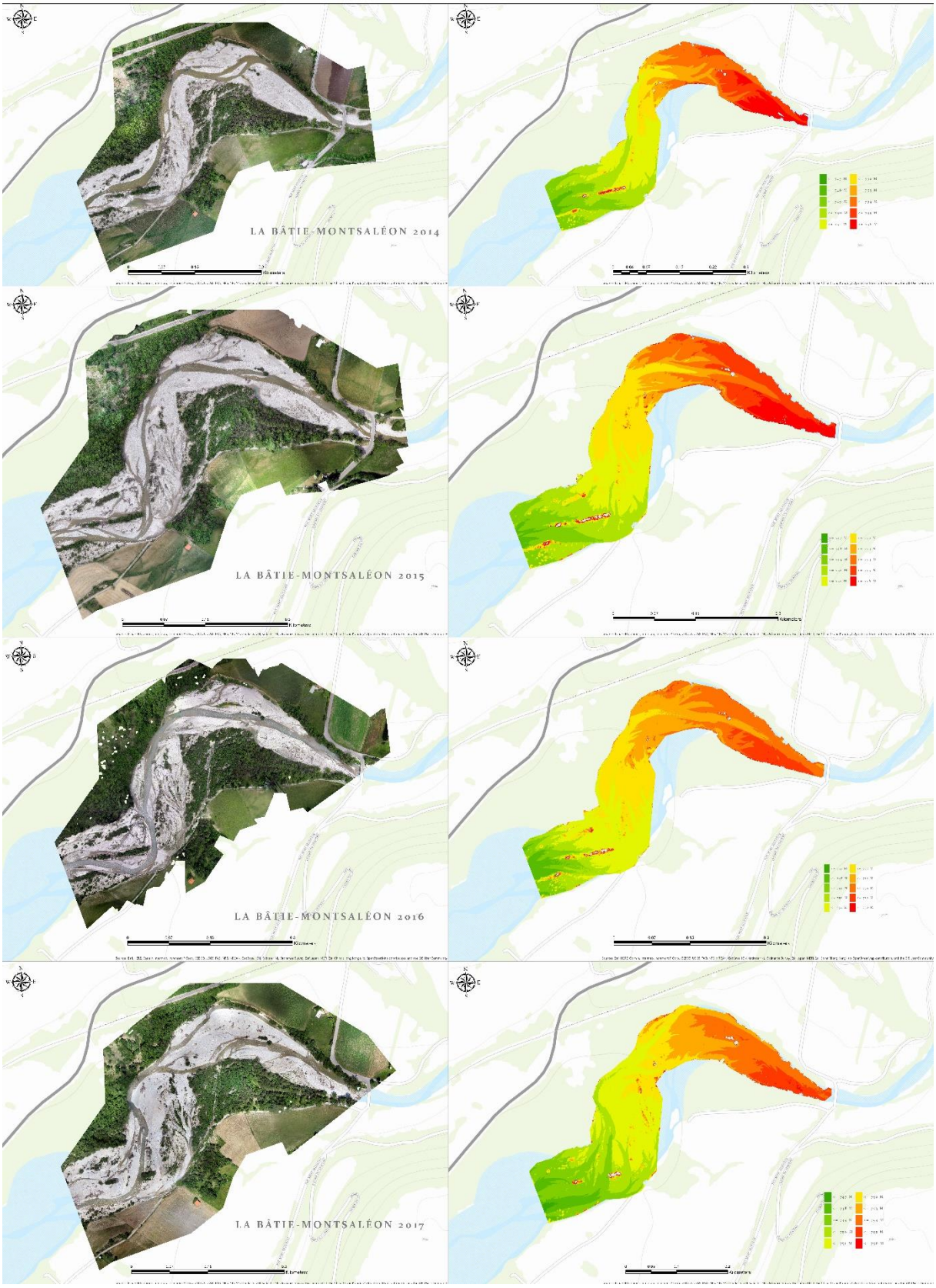

Figure 55 *La Bâtie-Montsaléon timeseries ("Stretched" and "Classify" classification method)*

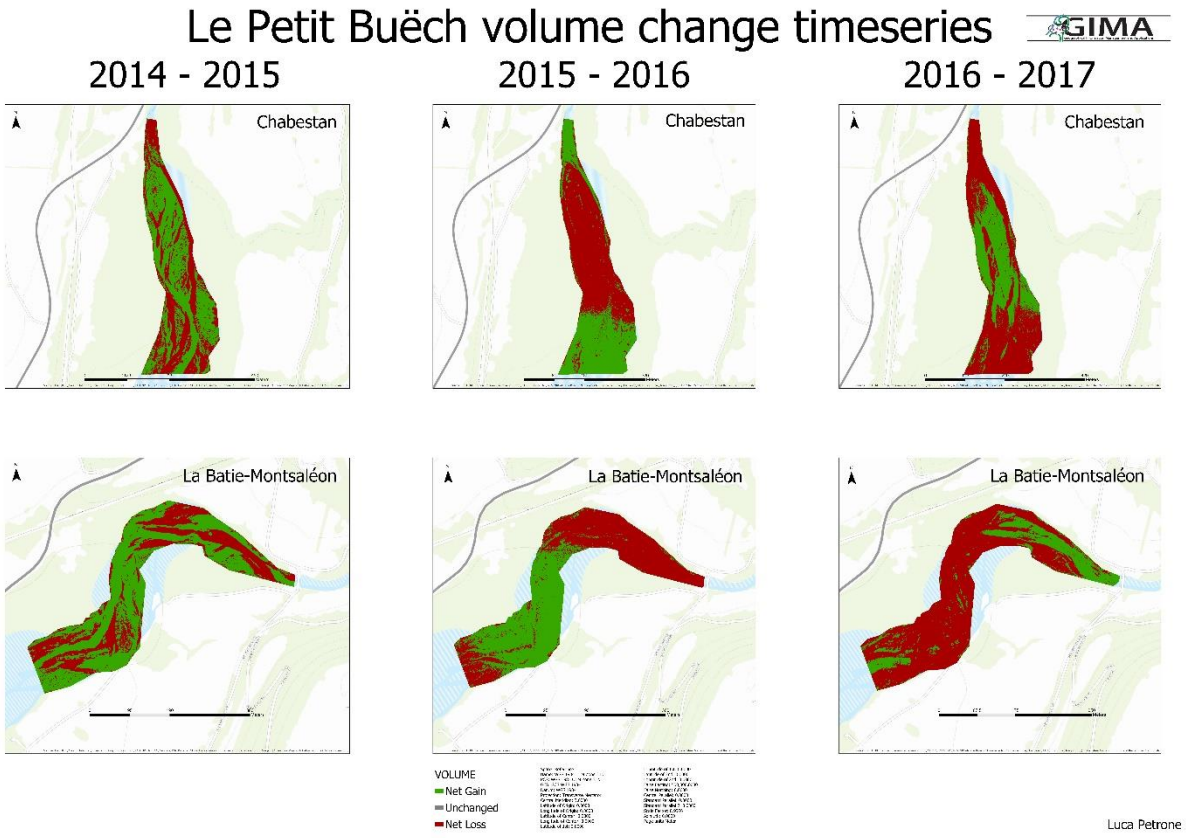

Figure 56 *Le Petit Buëch volume change timeseries*